PHYSICAL REVIEW D, VOLUME 65, 075025

Basis independent neutrino masses in the R_p violating minimal supersymmetric standard model

Sacha Davidson
Theoretical Physics, Oxford University, 1 Keble Road, Oxford OX1 3NP, United Kingdom

Marta Losada
Centro de Investigaciones, Universidad Antonio Nariño, Calle 59 No. 37-71, Santa Fe de Bogotá, Colombia
(Received 13 March 2001; published 5 April 2002)

We calculate the neutrino mass matrix up to one loop order in the minimal supersymmetric standard model without R parity, including the bilinears in the mass insertion approximation. This introduces additional diagrams usually neglected in the literature. We systematically consider the possible new diagrams, and find a few missing from our previous work. We provide analytic expressions for the mass matrix elements in the neutrino flavor basis, which are independent of the H_d-L_i basis choice in the Lagrangian. We compare the contributions from different diagrams, and make ''Lagrangian-basis-independent'' estimates of when the new diagrams need to be included. We briefly discuss the phenomenology of a toy model of bilinear R-parity violation.

DOI: 10.1103/PhysRevD.65.075025 PACS number(s): 12.60.Jv, 11.30.Pb, 14.60.Pq

I. INTRODUCTION

The construction of a model which generates neutrino masses [1] requires some extension of the standard model. A possibility is the minimal supersymmetric standard model (MSSM) [2,3] without R parity. The quantum number R_p is defined as $R_p=(-1)^{L+3B+2S}$, where L, B, S are the lepton and baryon number and the spin of the particle, respectively [4]. In a general R_p nonconserving supersymmetric (SUSY) version of the SM, the lepton number is not conserved,[1] which allows nonzero neutrino masses.

The main physical motivation for neutrino masses comes from the anomalous neutrino data from both solar and atmospheric neutrino experiments [5]. In the R-parity violating ($\not{R}_p$) MSSM, one neutrino can acquire a tree level mass through a seesaw effect from the mass matrix of the neutrinos and neutralinos [6]. In order that the rest of the neutrinos become massive, loop diagrams that violate the lepton number (by two units) must also be considered [7,8]. To generate neutrino masses that fit experimental constraints we must require that $\Delta m^2_{\mathrm{sun}} \lesssim 10^{-4}$ eV^2, $\Delta m^2_{\mathrm{atm}} \in [10^{-3},10^{-2}]$ eV^2. For solar neutrino data there are several different possibilities for the relevant mixing angle (large or small mixing angle solutions) while for atmospheric neutrinos the mixing angle must be in the range $\sin^2 2\theta_{\mathrm{atm}} \in [0.85,1]$.

The purpose of this paper is to provide *exact*, ''basis-independent'' neutrino mass matrix elements, which are given in Appendix B. As far as we know this is the first basis-independent exact calculation of all the finite one-loop diagrams that contribute to the neutrino mass matrix. We present complete analytic expressions for all of the diagrams, and clarify how the neutrino mass matrix elements can be ''basis independent.'' We discuss in detail when the different contributions to the neutrino mass matrix are relevant, identifying for both bilinear and trilinear contributions when they must be included or can be neglected. We also place bounds on the new combinations of couplings constants that contribute to the neutrino mass. We discuss phenomenological issues for a toy model where the R_p violation comes from the soft SUSY breaking sector of the potential. We will discuss phenomenology in more detail in a subsequent publication [10].

In the remainder of this section, we review our notation and previous work. In Sec. II we discuss what we mean by ''basis independent'' neutrino mass matrix elements, what we calculate, and how basis dependent it is. In Sec. III we discuss when the bilinears are important in the loop contributions to neutrino masses. This is a detailed discussion, with generation indices, of results presented in [11]. In Sec. IV we study the phenomenology of some simple bilinear models. We conclude in Sec. V. Appendix A discusses which are the relevant diagrams that we include in our calculations. In Appendix B the neutrino mass matrix elements are given in terms of MSSM parameters and basis-independent combinations of coupling constants that parametrize $\not{R}_p$. Additional Feynman rules for including $\not{R}_p$ in the mass insertion approximation can be found in Appendix C. Numerical bounds on R-parity violating parameters obtained from the different diagrams are given in Appendix D.

In the MSSM, the down-type Higgs superfield and the lepton doublet superfields have the same gauge quantum numbers, which means that they can mix if the lepton number is not conserved. Thus, we can construct a vector $L_J=(H_d,L_i)$ with J:4.1. With this notation, the superpotential for the supersymmetric SM with the R_p violation can be written as

$$W=\mu^J H_u L_J+\frac{\lambda^{JKl}}{2}L_J L_K E^c_l+\lambda'^{Jpq}L_J Q_p D^c_q + h_t^{pq} H_u Q_p U^c_q. \quad (1)$$

We contract SU(2) doublets with $\varepsilon_{\alpha\beta}$: $\varepsilon_{11}=\varepsilon_{22}=0$, $\varepsilon_{12}=-\varepsilon_{21}=-1$. The R_p violating and conserving coupling constants have been assembled into vectors and matrices in L_J space: we call the usual μ parameter μ_4, and identify h_e^{jk}

[1]Baryon number is also in general not conserved; however, we will impose baryon number conservation by hand to avoid proton decay constraints, see, e.g., [9]

$=\lambda^{4jk}$,[2] and $h_d^{pq}=\lambda'^{4pq}$. We call the usual $\not{R}_p$ mass $\epsilon_i=\mu_i$. Lower case roman indices i,j,k and p,q are lepton and quark generation indices. We frequently suppress the capitalized indices, writing $\vec{\mu}=(\mu_4,\mu_3,\mu_2,\mu_1)$. We also include possible R_p-violating couplings among the soft SUSY breaking parameters, which can be written as

$$V_{soft}=\frac{\tilde{m}_u^2}{2}H_u^\dagger H_u+\frac{1}{2}L^{J\dagger}[\tilde{m}_L^2]_{JK}L^K+B^J H_u L_J+A^{ups}H_u Q_p U_s^c + A^{Jps}L_J Q_p D_s^c+\frac{A^{JKl}}{2}L_J L_K E_l^c+\text{H.c.} \tag{2}$$

Note that we have absorbed the superpotential parameters into the A and B terms, e.g. we write $B^4 H_u H_d$ not $B^4\mu^4 H_u H_d$. We abusively use capitals for superfields [as in Eq. (1)] and for their scalar components.

In this notation where the Higgs boson joins the leptons as the fourth direction in $\{L_I\}$ space, the relative magnitude of R_p violating and conserving coupling constants vary with the choice of the Higgs direction. R_p violation can be understood geometrically: if all interactions in the Lagrangian agree which direction is the Higgs boson (e.g. $\hat{H}=\hat{L}_4$), then R_p is a good symmetry. But if there is misalignment in $\{L_I\}$ space between different couplings constants (for instance $\lambda'^{ipq}\neq 0$ in the basis where $\mu_1=\mu_2=\mu_3=0$) then R_p is not conserved. This $\not{R}_p$ can be parametrized by basis independent combinations of coupling constants [6,12–14]. These invariant measures of R_p violation in the Lagrangian are analogous to Jarlskog invariants which parametrize CP violation.

Early work on $\not{R}_p$ neutrino masses [7] used models where the bilinear $\not{R}_p$ could be rotated out of the mass terms ($B_i,\mu_i,\tilde{m}_{4i}^2$, referred to as "bilinears") into the trilinear interactions. Most subsequent analytic estimates [24] have followed the calculation of [7] and neglected the $\not{R}_p$ bilinear masses in the loop contributions to the neutrino masses. This does not generate the complete set of one loop diagrams contributing to $[m_\nu]_{ij}$, so it is formally inconsistent. It would be acceptable if neglecting the bilinear contributions corresponded to neglecting loops suppressed by some additional small parameter. However, the size of the bilinears is basis dependent, so what is neglected depends on the basis choice, and this basis dependence of neutrino masses has caused some confusion in the literature.

In a previous paper [11], we systematically analyzed $\Delta L=2$ loop contributions to neutrino masses in the mass insertion approximation [15]. This led us to identify new diagrams which have not been included in many analytic estimates in the literature. We gave basis-independent *estimates* for all diagrams using a common SUSY scale for all R-parity conserving mass parameters, and calculated the neutral loop diagram exactly (Grossman-Haber diagram). We found that Grossman and Haber had neglected diagrams in their calculation, suggesting that an exact basis-independent calculation would be worthwhile. The mass insertion approximation is valid as we know experimentally that neutrino masses are small. It is a particularly transparent way to include the bilinears, because the $\not{R}_p$ Feynman rules can be read off the Lagrangian, and all the $\not{R}_p$ appears perturbatively in the numerator ("upstairs") of each contribution. The relative contributions of different diagrams are easy to see. The main point of our previous paper was that the issue of the basis choice for calculating neutrino masses is transparent if we keep all contributions.

The bilinear $\not{R}_p$ contribution to loops, as well as at the tree level, has been included in [16–18], where neutrino masses are obtained, after the exact diagonalization of the mass matrices of all particles which propagate in the $\Delta L=2$ loops. The bilinears mix standard model and SUSY particles, generating mass matrices of large dimension, so these results are partially numerical. They propagate tree-level mass eigenstates in their loop diagrams. The discussion in Ref. [18] includes gauge loops. Reference [17] has approximate diagonalization formulas, calculated in the seesaw approximation, which is equivalent to the mass insertion approximation used here; they have few diagrams and long mixing angle formulas, whereas we have more diagrams and only MSSM mixing angles.

II. ISSUES OF BASIS

There is no unique interaction eigenstate basis for the $Y=-1$ fields (the components of the L_i and H_d superfields) in the $\not{R}_p$ MSSM. This means that the Lagrangian parameters depend on an arbitrary choice of basis, or equivalently that Lagrangians which differ by a rotation in $\{L_I\}$ space make equivalent physical predictions. Observables cannot depend on the choice of basis in the Lagrangian $\mathcal{L}$, so they must be scalar functions of the vector and tensor parameters in $\{L_I\}$ space. It is common in SUSY to study the dependence of physical observables on Lagrangian inputs. The basis dependence of the Lagrangian makes this problematic in $\not{R}_p$ models because a point in physical parameter space corresponds to different numerical inputs in different bases. So comparing results calculated in different bases is difficult.

The $\not{R}_p$ in the Lagrangian can be parametrized in a basis independent way by combining coupling constants, masses and vacuum expectation values (vectors and matrices in $\{L_I\}$ space) into scalar "invariants," which are zero when R_p is conserved. Physical observables can be expressed in terms of these invariants and other R_p conserving quantities. For a discussion of constructing invariants, see e.g. [12,11,14,19].

Neutrino masses and mixing angles are measurable quantities, so they must be *independent* of the basis choice in the *Lagrangian*. However, note that the mixing angles parametrize the rotation between the neutrino and charged lepton mass eigenstate bases in lepton flavor space, so are defined in terms of *physical* bases. This "basis dependence" cannot be avoided. We will therefore present *Lagrangian basis independent* formulas for neutrino mass matrix elements $[m_\nu]_{ij}$ in the charged lepton mass eigenstate basis. The neutrino masses and mixing angles can be computed from $[m_\nu]_{ij}$ in

[2]We have changed convention with respect to factors of 2 in λ from our previous paper: we now put $\lambda/2$ in the superpotential, with $\lambda^{4ij}=h_e^{ij}$.

TABLE I. The basis-independent invariants used to parametrize the $\not R_p$ relevant for neutrino masses. They are zero if R_p is conserved. δ_μ and δ_B parametrize bilinear $\not R_p$. Note that these invariants have signs: for arbitrary vectors $\vec{a}$ and $\vec{b}$, $\vec{a}\cdot\lambda^i\cdot\vec{b}=-\vec{b}\cdot\lambda^i\cdot\vec{a}$.

$\delta_\mu^i \equiv \dfrac{\vec{\mu}\cdot\lambda^i\cdot\vec{v}}{\lvert\vec{\mu}\rvert\sqrt{2}m_e^i}$	$\delta_B^i \equiv \dfrac{\vec{B}\cdot\lambda^i\cdot\vec{v}}{\lvert\vec{B}\rvert\sqrt{2}m_e^i}$
$\delta_{\lambda'}^{ipq} \equiv \dfrac{\vec{\lambda}'^{pq}\cdot\lambda^i\cdot\vec{v}}{\sqrt{2}m_e^i}$	$\delta_\lambda^{ijk} \equiv \dfrac{\vec{v}\cdot\lambda^i\lambda^k\lambda^j\cdot\vec{v}}{2m_e^i m_e^j}$

this basis, so it contains all the measurable information. At first sight, it may appear self-contradictory to compute so-called basis-independent formulas for mass matrix elements $[m_\nu]_{ij}$ which depend on the basis in which they are computed. The crucial point is that we want formulas for physically measurable quantities, and we want those formulas to be independent of the arbitrary choice of interaction eigenstate basis in the Lagrangian. The $[m_\nu]_{ij}$ are physical—they can be calculated from the Maki-Nakagawa-Sakata (MNS) matrix and the neutrino masses—and Lagrangian basis-independent.

The flavor basis can be written in terms of vacuum expectation values (VEV) and coupling constants, so neutrino mass matrix elements in this basis are proportional to invariants. We list the four invariants relevant for neutrino masses in Table I. The flavor basis is

$$\hat{H}_d=\frac{\vec{v}}{v}$$

$$\hat{L}^i=\frac{\lambda^i\cdot\vec{v}}{\lvert\lambda^i\cdot\vec{v}\rvert}, \tag{3}$$

where $\vec{v}$ is the vector of vacuum expectation values in the down-type Higgs sector and we impose the requirement that $\vec{v}\cdot\lambda^i\cdot\lambda^j\cdot\vec{v}\propto\delta^{ij}$. The lower case index labeling the matrix λ^k is the singlet lepton index: $[\lambda^k]_{IJ}=\lambda^{IJk}$. So there are three flavor eigenstates $\hat{L}^i$ in $\{L_I\}$ space: $\hat{L}_J^i=\lambda^{JKi}v_K/\sqrt{v_P\lambda^{NPi}\lambda^{NMi}v_M}$ (no sum on i).[3] This corresponds to the charged lepton mass eigenstate basis in the absence of $\not R_p$. In this R_p-conserving case $\lambda^{4ij}=h_e^{ij}$ and $\lambda^{kij}=0$, where k,i,j:1.3. So $\lambda^{IJk}v_I=\sqrt{2}m_e^{jk}$ ($I=4,J=j$:1.3), $\vec{v}\cdot\lambda^i\cdot\lambda^j\cdot\vec{v}\propto\delta^{ij}$ is the condition that the $\{e_R^c\}$ are in the mass eigenstate basis, and $\lambda^i\cdot\vec{v}$ are the charged doublet eigenvectors. In the presence of bilinear $\not R_p$, the basis (3) will not be exactly the charged lepton mass eigenstate basis. However, bilinear $\not R_p$ masses are required to be small by neutrino masses, so the basis (3) is close to the charged lepton mass eigenstate basis. The smallness of such δ_μ^i terms is crucial. We get basis independent formulas because we include the $\not R_p$ masses as well as couplings in perturbation theory. Our results are basis independent to order ($\not R_p$ coupling)^2, and neglect higher order effects such as the difference between basis (3) and the exact charged lepton mass eigenstate basis. We are also neglecting the R conserving contributions to squark and slepton flavor mixing matrices due to R-parity violating (RPV) parameters [20], as their effect is order δ^4. This makes them irrelevant, since neutrino masses are $\propto\delta^2$. The $\not R_p$ couplings which do not contribute to neutrino masses at order ($\not R_p$ coupling)^2 should give the most significant contributions to m_ν at order ($\not R_p$ coupling)^4, as phenomenologically these couplings can be larger.

[3]The capitalized index ordering on λ^{NPi} is because $\vec{a}\cdot\lambda\cdot\vec{b}=-\vec{b}\cdot\lambda\cdot\vec{a}$ is an antisymmetric product. The transpose of $\hat{L}^i$ is $-\vec{v}\cdot\lambda^i/\lvert\vec{v}\cdot\lambda^i\rvert$.

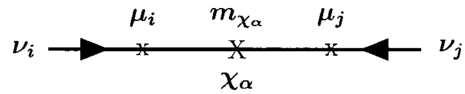

FIG. 1. Tree-level neutrino mass in the mass insertion approximation.

A significant advantage of the basis-independent formalism is that the neutrino masses can be computed in any Lagrangian basis, including those where the mass insertion approximation is not valid. This could be easier than rotating to the $\langle\tilde{\nu}_i\rangle=0$ basis, because the VEV is a derived quantity, calculated by minimizing the potential. For instance, consider a model where all the $\not R_p$ is in $\vec{B}$ and $\vec{v}$—that is, there is a basis where all the $\not R_p$ couplings other than B_i and $\langle\tilde{\nu}_i\rangle$ are zero. Clearly it is easier to evaluate invariants in this basis than to rotate to $\langle\tilde{\nu}_i\rangle=0$. The basis independent formalism also makes it simple to compare results computed in different bases.

We include the $\not R_p$ bilinears and the $A+\mu\tan\beta$ scalar masses in the mass insertion approximation. This means that we treat *all* the $\not R_p$ couplings and masses in perturbation theory, following the same approach as in Ref. [11]. We propagate MSSM mass eigenstates (neglecting the scalar doublet-singlet mixing masses, which we include in the mass insertion approximation).

The tree level neutrino mass is non-zero if $\delta_\mu\neq 0$ [6]. The diagram appears in Fig. 1 in the mass insertion approximation. In the basis of Eq. (3), it contributes a mass matrix

$$[m_\nu]_{ij}^{tree}=-(\vec{\mu}\cdot\hat{L}_i)\sum_\alpha\frac{Z_{\alpha3}^*Z_{\alpha3}^*}{m_{\chi_\alpha}}(\vec{\mu}\cdot\hat{L}_j), \tag{4}$$

which gives a mass $m_3^{tree}=\Sigma_{i,\alpha}(\delta_\mu^i)^2 Z_{\alpha3}^{*2}\lvert\mu\rvert^2/m_{\chi_\alpha}$ to the neutrino

$$\hat{\nu}_3^{tree}=\frac{\delta_\mu^i}{\delta_\mu}\hat{L}_i, \tag{5}$$

where $\delta_\mu=\sqrt{\Sigma_i(\delta_\mu^i)^2}$, and the neutralino index α runs from 1 to 4. The index "3" on Z corresponds to the interaction eigenstate $\tilde{h}_u$—see Appendix C for our conventions on Z.

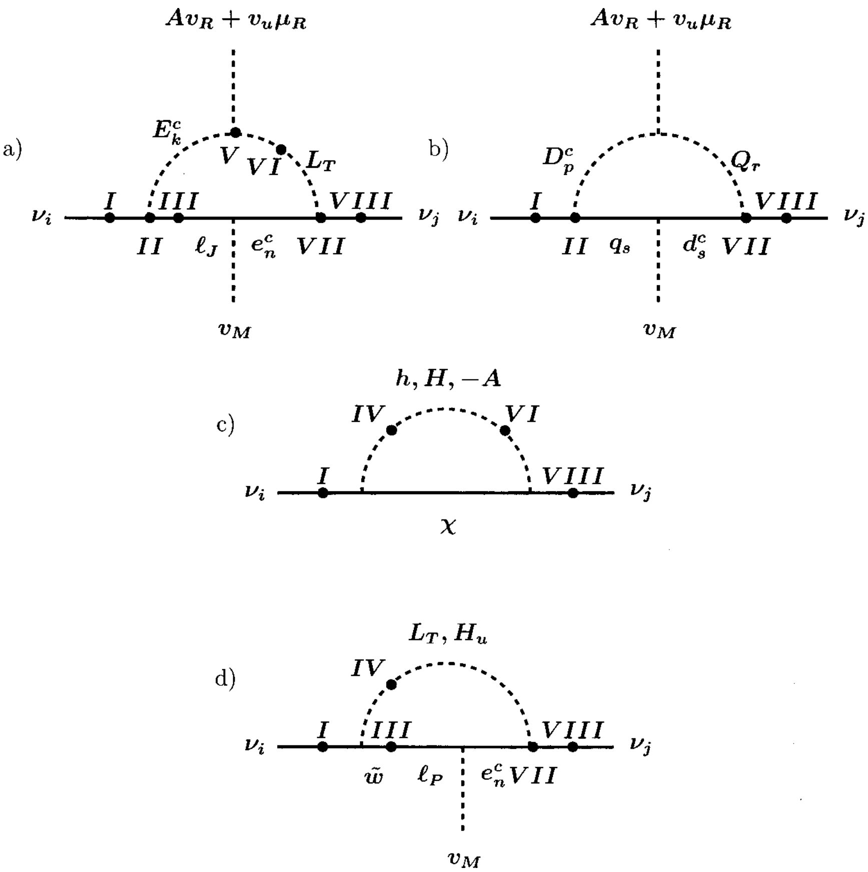

FIG. 2. Schematic representation of one-loop diagrams contributing to neutrino masses. The filled circles indicate possible positions for $\not{R}_p$ interactions, which can be trilinears (at positions II and VII) or mass insertions. The misalignment between $\vec{\mu}$ and $\vec{v}$ allows a mass insertion on the lepton/Higgsino lines (at points I, III, or VIII) and at the A term on the scalar line (position V). The soft $\not{R}_p$ masses appear as mass insertions at positions VI and IV on the scalar line. (a) corresponds to the charged loop with trilinear couplings λ (or h_e) at the vertices. (b) is the colored loops with trilinear λ' or Yukawa h_b couplings. (c) is the neutral loops with two gauge couplings, and (d) corresponds to the charged loop with one gauge and a Yukawa coupling. This diagram occurs if gauginos mix with charged leptons—that is if $\delta_\mu \neq 0$. See also Fig. 3.

Equation (4) is equivalent to the usual formula $m_\nu^{tree} = \det[M^{(5)}]/\det[M^{(4)}]$, where $M^{(5)}$ ($M^{(4)}$) is the $\not{R}_p$ 5×5 neutralino and neutrino mass matrix (MSSM neutralino mass matrix), as can be seen by writing $M^{(5)}$ and $M^{(4)}$ in the MSSM mass eigenstate basis with $\langle\tilde{\nu}_i\rangle = 0$.

Loop corrections to the neutrino mass matrix can be divided into three categories. First, there are gauge and top Yukawa coupling loops which renormalize the mass of ν_3^{tree}—we neglect these because their effect is small [16]. Second, there are loop corrections to δ_μ^i (equivalently, μ_i and/or $\langle\tilde{\nu}_i\rangle$) which can modify the direction of $\hat{\nu}_3$—these we partially compute and list in the Appendixes. They are renormalization scale dependent, because they are loop corrections to the tree mass. We are not interested in loop corrections to the tree mass, so we rotate these away. This is discussed in more detail in Appendix A. Finally, there are finite loops which give mass to any neutrino. The third group has the most interesting loops, because they generate mass for the two neutrinos who are massless at the tree level. Schematic representations of the one-loop neutrino mass diagrams that we consider are reproduced in Fig. 2. This is a slightly modified version of a figure from Ref. [11]. Each of the four diagrams represents a number of Feynman diagrams. This should be an almost[4] complete set of one loop, $\Delta L = 2$ diagrams which generate mass matrix elements for the neutrinos that are massless at tree level. The possible places on the diagram for the two required lepton number violating interactions are labeled I . . . VIII. With the definition $\hat{H}\propto\vec{v}$, lepton number violation is not possible at the charged lepton mass insertion in diagrams 2(a) and 2(d). (An sneutrino VEV could provide lepton number violation at this point in a basis where $\langle\tilde{\nu}_i\rangle \neq 0$.)

In Appendix B we list all the possible loop diagrams, giving exact formulas in a basis-independent way for each diagram's contribution to $[m_\nu]_{ij}$. In Table II we summarize the diagrams for the reader's benefit and make basis independent estimates by setting all the heavy masses to a unique scale m_{SUSY}. The lists start with the canonical trilinear diagrams, then the Grossman-Haber loop induced by the soft bilinears, and finally all the additional diagrams which arise when the bilinear δ_μ^i are included in the loops. For each diagram, labeled by $a \rightarrow d$ for the diagram category of Fig. 2, and by roman numeral identifying where the $\not{R}_p$ should appear on the figure, we give an estimate of the diagram in terms of the invariants listed in Table I. We have added a few relevant diagrams missing from the list in [11].

To evaluate diagram 2(b) with $\not{R}_p$ at points II and VII (this is the usual colored trilinear diagram), we identify the external neutrino legs as $\hat{L}_i$ and $\hat{L}_j$. At vertices II and VII sit couplings $\vec{\lambda}'^{sq}D_{qp}$ and $\vec{\lambda}'^{ts}Q_{tr}$. (The λ' indices are in the quark mass eigenstate basis, and the matrices D and Q diagonalize the singlet and doublet squark mass matrices—see Appendix C.) The diagram is therefore

[4]We discuss in Appendix B why we neglect certain finite diagrams of the third type.

TABLE II. Estimated contributions to $[m_\nu]^{ij}$ from all the diagrams. In the second two columns are the label of the diagram of Fig. 2, and the position on the diagram of the two $\Delta L = 1$ interactions. Column four is the ‘‘basis independent’’ estimated contribution to the neutrino mass matrix in the flavor basis. All indices other than i and j are summed.

No.	Diagram	Position of $\not{R}_p$	$16\,\pi^2 m_{SUSY}[m_\nu]^{ij}$
1	a	II VII	$\delta_\lambda^{ink}\delta_\lambda^{jkn} m_{e_n} m_{e_k}$
2	b	II VII	$3\delta_{\lambda'}^{iqq}\delta_{\lambda'}^{jqq}(m_{d_q})^2$
3	c	IV VI	$g^2\delta_B^i\delta_B^j m_\chi m_{SUSY}/4$
4	b	I VII + II VIII	$3(\delta_\mu^i\delta_{\lambda'}^{jqq}+\delta_\mu^j\delta_{\lambda'}^{iqq})(m_{d_q})^2 h_d^q$
5	a	II VI	$\delta_\lambda^{ijk} m_{e_k}\delta_B^k(m_{e_j}h_e^j - m_{e_i}h_e^i)$
6	a	I VII + II VIII	$(\delta_\mu^i\delta_\lambda^{jkk}+\delta_\mu^j\delta_\lambda^{ikk})(m_{e_k})^2 h_e^k$
7	a	I V	$\delta_\mu^i\delta_\mu^j[(m_{e_j}h_e^j)^2+(m_{e_i}h_e^i)^2]$
8	a	II V	$\delta_\lambda^{ijk}\delta_\mu^k m_{e_k}(h_e^i m_{e_i} - h_e^j m_{e_j})$
9	a	III V	$\delta_\mu^i\delta_\mu^j m_{e_j} m_{e_i} h_e^i h_e^j$
10	a	III VIII	$\delta_\mu^i\delta_\mu^j[(m_{e_i}h_e^i)^2+(m_{e_j}h_e^j)^2]$
11	a	I VI	$\delta_\mu^i\delta_B^j(m_{e_j}h_e^j)^2+\delta_\mu^j\delta_B^i(m_{e_i}h_e^i)^2$
12	a	III VII	$\delta_\lambda^{jin}\delta_\mu^n m_{e_n}(m_{e_j}h_e^j - m_{e_i}h_e^i)$
13	a	III VI	$(\delta_B^i\delta_\mu^j h_e^j h_e^i m_{e_i} m_{e_j}+\delta_B^j\delta_\mu^i h_e^i h_e^j m_{e_j} m_{e_i})$
14	d	III IV	$g[\delta_B^i\delta_\mu^j(m_{e_j})^2+\delta_B^j\delta_\mu^i(m_{e_i})^2]$
15	d	III VIII	$g\delta_\mu^i\delta_\mu^j[(m_{e_i})^2+(m_{e_j})^2]$
16	d	I III	$g\delta_\mu^i\delta_\mu^j[(m_{e_i})^2+(m_{e_j})^2]$
17	d	I VII	$g m_{e_k} m_{SUSY}(\delta_\mu^i\delta_\lambda^{jkk}+\delta_\mu^j\delta_\lambda^{ikk})$
			$3g m_{d_k} m_{SUSY}(\delta_\mu^i\delta_{\lambda'}^{jkk}+\delta_\mu^j\delta_{\lambda'}^{ikk})$
18	d	III VII	zero for degenerate sleptons
19	c	I VI+IV VIII	$g^2 m_{SUSY}^2(\delta_B^i\delta_\mu^j+\delta_\mu^i\delta_B^j)/4$
20	d	I V	$g\delta_\mu^i\delta_\mu^j[(m_{e_i})^2+(m_{e_j})^2]$
21	d	I IV	$g[\delta_\mu^i\delta_B^j(m_{e_j})^2+\delta_\mu^j\delta_B^i(m_{e_i})^2]$

$$[m_\nu]_{kj} = -3\sum_{s,q,p,r,t,x,y}(i\hat{L}_k\cdot\vec{\lambda}'^{sq})D_{qp}Q_{tr}(i\vec{\lambda}'^{ts}\cdot\hat{L}_j)(iQ^*_{yr}|\tilde{A}_d^{yx}|D^*_{xp})(-|m_{d_s}|)$$

$$\times\int\frac{d^4k}{(2\pi)^4}\frac{i}{k^2-m^2_{\tilde{D}^c_p}}\frac{i}{k^2-m^2_{\tilde{Q}_r}}\frac{i}{k^2-m^2_{d_s}}+(k\leftrightarrow j)$$

$$= -\frac{3}{16\pi^2}\sum_{s,p,r,q,t,x,y}\lambda'^{ksq}D_{qp}Q_{tr}\lambda'^{jts}\lambda'^{Mss}\frac{v_M}{\sqrt{2}}Q^*_{yr}\left[(\lambda A)'^{Rxy}\frac{v_R}{\sqrt{2}}+\frac{v_u}{\sqrt{2}}\mu_R\lambda'^{Rxy}\right]D^*_{xp}I(m_{\tilde{Q}_r},m_{\tilde{D}^c_p},m_{d_s})+(k\leftrightarrow j) \tag{6}$$

$$= -\frac{3}{16\pi^2}\sum_{s,p,r,q,t,x,y}\delta_{\lambda'}^{ksq}\delta_{\lambda'}^{jts}D_{qp}D^*_{xp}Q_{tr}Q^*_{yr}I(m_{\tilde{Q}_r},m_{\tilde{D}^c_p},m_{d_s})|\tilde{A}_d^{xy}||m_{d_s}|+(k\leftrightarrow j) \tag{7}$$

$$\sim -\frac{3\delta_{\lambda'}^{ksp}\delta_{\lambda'}^{jps}}{8\pi^2}\frac{|m_{d_s}m_{d_p}|}{m_{SUSY}}, \tag{8}$$

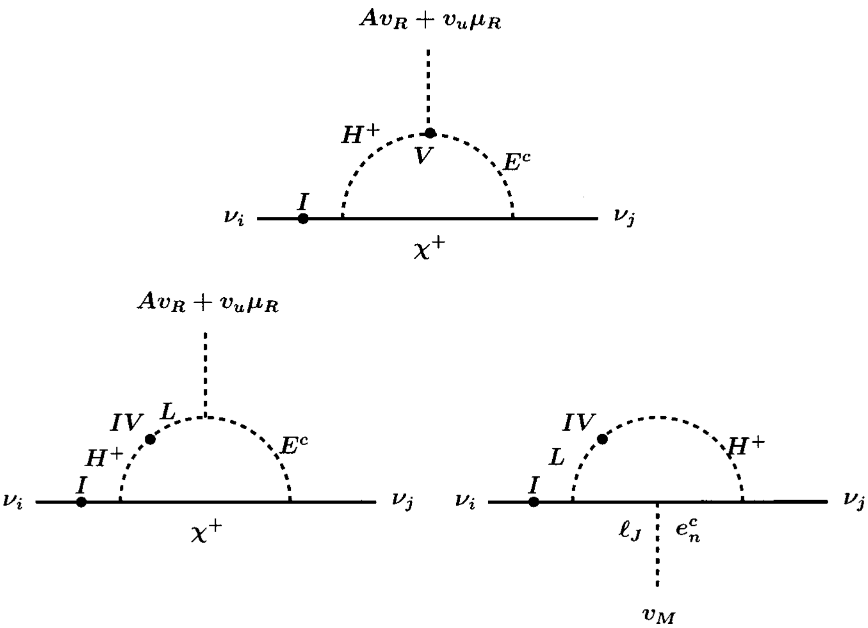

FIG. 3. Some of the charged $g-\lambda$ loops differ slightly from Fig. 2(d). The loops with R-parity breaking at I,V and at I,IV are shown here with the correct particle labels.

where $\tilde{A}^{pr} = -[(A\lambda')^{Rpr} v_R + v_u \mu_R \lambda'^{Rpr}]$, and we work in the down quark mass eigenstate basis: $\overrightarrow{\lambda'^{st}} \cdot \vec{v}$ is diagonal. The integrals I are listed in Appendix B. The last line corresponds to the last column of Table II. Note that we do not divide by 2 when we symmetrize on i and j, because the diagram with $i \leftrightarrow j$ is different. This agrees with [17,18][5] and disagrees with [8]. It is clear in the mass insertion approximation that one should not divide by 2, because in one case ν_i couples to $\tilde{D}^c$ and in the other case to $\tilde{Q}$. In the mass eigenstate formalism, one can see that these are distinct diagrams not included in the sum over p,r,s by considering the case where only λ'^{132} and λ'^{223} are non-zero.

In our previous paper we were unclear about whether the charged goldstone boson of SU(2) could mix with the $\{E^c\}$. This was due to various sign discrepancies in the literature. As expected, the goldstone is pure SU(2)—so there is no loop diagram propagating a W^μ that is proportional to a gauge times a Yukawa coupling.

III. WHEN ARE THE BILINEARS IMPORTANT IN LOOPS?

Bilinear contributions to loops have traditionally been neglected, which intuitively seems reasonable if they are "small" in a "sensible" basis close to the MSSM mass eigenstate basis. However, this apparently reasonable oversight is confusing, because the size of what is neglected depends on the basis choice. In this section we provide basis-independent conditions for when the bilinears can be neglected in the loops—assuming the mass matrix elements are then calculated in a sensible basis where the bilinears are small. These are not hard and fast rules, but estimates of when the extra bilinear diagrams should be included.

A slightly different approach would be to consider the relative size of all the diagrams, and catalogue all the permutations of which diagrams should be included and which neglected. For instance, it is possible that the trilinears are negligible with respect to the bilinear diagrams, or that the λ trilinear contributes only a small correction to the λ' trilinear, and can be ignored. Here we assume that the trilinear contributions are always calculated, because they take little effort. Then we ask whether δ_B should also be included—this is a few more diagrams. Finally we consider adding the δ_μ contributions, which is many more diagrams. We do not specifically discuss the case where δ_μ should be included but the δ_B contributions are insignificant, because the δ_B diagrams are relatively little work compared to the many δ_μ diagrams.

In our previous paper, we outlined three cases:

Case A: all the bilinear contributions to loop diagrams are negligible. In this case the loop contributions to the neutrino mass matrix are the usual trilinear diagrams of Figs. 2(a) and 2(b).

Case B: δ_μ is negligibly small, but δ_B should be included. In addition to the diagrams of case A, one should consider the neutral Grossman-Haber loop of Fig. 2(c), and possibly the δ_B mass insertion to Fig. 2(a).

Case C: Include all bilinear $R\!\!\!/_p$ contributions. There are additional contributions to diagrams in Figs. 2(a), 2(b), and 2(c), and new diagrams in Fig. 2(d) and Fig. 3.

We determine basis-independent criteria for when the bilinears can be neglected in the loops by comparing our estimates of the size of each diagram from the last column of Table II. A diagram should be included if its contribution is

[5]We thank E.J. Chun for a discussion of this point.

of order of the trilinear loops—however, we want to avoid comparing bilinear loop corrections of the tree mass (which are irrelevant), with the trilinear loops contributing masses to neutrinos which are massless at tree level. So we distinguish two cases: $m^{tree} \lesssim m^{loop}$, and $m^{tree} \gg m^{loop}$.

If $m^{tree} \lesssim m^{loop}$, we simply compare bilinear to trilinear loop mass matrix elements. Since δ^i_μ is not large enough to produce $m^{tree} \gtrsim m^{loop}_{ij}$, it is negligible in the loops, so we are in case A or B.

If $m^{tree} \gg m^{loop}$, we consider only the loop mass matrix for the neutrinos that are massless at tree level. We compare the bilinear and trilinear contributions to this sub-matrix. Cases A, B, or C can arise if $m_3^{tree} \gg m^{loop}$.

A. Case B—including the soft bilinear B_i

We first consider when δ_B should be included in the loops. The Grossman-Haber (GH) loop is of order[6] $m_\nu^{ij} \sim g^2 \delta_B^i \delta_B^j m_\chi/(64\pi^2)$, which is potentially large because it is proportional to gauge rather than Yukawa couplings. Recall that the canonical trilinear diagrams are of order $m_\nu^{ij} \sim \delta_{\lambda'}^{i33} \delta_{\lambda'}^{j33} m_b^2/(8\pi^2 m_{SUSY})$.

If the tree mass is small, $m^{tree} \lesssim m^{loop}$, then the Grossman-Haber loop should be included if it is of order the trilinear loop. This will occur if

$$\frac{g}{2}\delta_B^j \gtrsim \delta_{\lambda'}^{jqp}\sqrt{h_d^q h_d^p}, \quad \delta_\lambda^{jkl}\sqrt{h_e^k h_e^l}, \tag{9}$$

or the condition to neglect δ_B can be roughly estimated as

$$\delta_B^j \ll \delta_{\lambda'}^{j33} h_b, \delta_\lambda^{j33} h_\tau \quad (m^{tree} \lesssim m^{loop}). \tag{10}$$

Alternatively, if $m^{tree} \gg m^{loop}$, we are only interested in the loop contributions to the mass of neutrinos ν_2 and ν_1 who are massless at tree level: if $\vec{B}$ is aligned with $\vec{\mu}$, then the GH loop is a correction to the tree-level mass, and can be neglected along with other such loops. $\vec{B}$ can be decomposed in components parallel and perpendicular to μ:

$$\vec{B} = \vec{B}_\perp + \vec{B}_\parallel, \tag{11}$$

with $\vec{B}_\parallel = (\vec{B}\cdot\vec{\mu})\vec{\mu}/|\vec{\mu}|^2$. The part of the Grossman-Haber loop proportional to $\delta^i_{B_\parallel}\delta^j_{B_\parallel}$ is a loop correction to the tree mass m^{tree}. The $\delta^i_{B_\parallel}\delta^j_{B_\perp}$ terms mix ν^{tree} with ν_2 and ν_1, so induce a "seesaw" mass for ν_1 and/or ν_2 which is negligible for $m^{tree} \gg m^{loop}$ [see the related discussion following Eq. (18)]. The mass matrix from the GH loop for ν_1 and ν_2 is therefore

$$[m_\nu]_{ij} \propto \frac{\delta^i_{B_\perp}\delta^j_{B_\perp}}{64\pi^2} m_\chi. \tag{12}$$

This will be comparable to or greater than the trilinear loops when

$$\frac{g}{2}\delta^i_{B_\perp} = \frac{g}{2}\left(\delta^i_B - \frac{\vec{B}\cdot\vec{\mu}}{|\vec{B}||\vec{\mu}|}\delta^i_\mu\right) \gtrsim \delta^{jqp}_{\lambda'_\perp}\sqrt{h_d^q h_d^p}, \quad \delta_\lambda^{jkl}\sqrt{h_e^k h_e^l}. \tag{13}$$

We define $\delta^{jqp}_{\lambda'_\perp} = \delta^{jqp}_{\lambda'} - \delta^j_\mu(\vec{\lambda}'^{qp}\cdot\vec{\mu})/|\vec{\mu}|$. This translates roughly into the condition that δ_B can be neglected in the loops if

$$\delta^i_{B_\perp} \ll \delta^{i33}_{\lambda'_\perp} h_b, \delta^{i33}_\lambda h_\tau \quad (m_\nu^{tree} \gg m_\nu^{loop}). \tag{14}$$

B. Case C—including μ_i

The tree-level neutrino mass is $\sim \Sigma_i (\delta^i_\mu)^2 m_\chi$, so if δ^i_μ is relevant in the loops, then $m^{loop} \ll m^{tree}$. The additional diagrams proportional to δ^i_μ should be included if they induce a loop mass for ν_2 and ν_1 greater than or of order the trilinear or GH loops.

We first consider the various δ^i_μ contributions to diagrams (a) and (d) of Fig. 2 which are of order $\sim[\delta^i_\mu (h^i_e)^2][\delta^j_\mu (h^j_e)^2] m_{SUSY}$. Generically the vector $(\delta^\tau_\mu h^\tau h^\tau,\ \delta^\mu_\mu h^\mu h^\mu,\ \delta^e_\mu h^e h^e)$ will not be aligned with $(\delta^\tau_\mu, \delta^\mu_\mu, \delta^e_\mu)$, so the δ_μ bilinear contributions should be included if

$$\delta^i_\mu (h^i_e)^2 \gtrsim \delta^{jkl}_\lambda \sqrt{h^k_e h^l_e}, \delta^{jpq}_{\lambda'_\perp}\sqrt{h^p_d h^q_d},$$
$$i,j,k,l,p,q \text{ not summed.} \tag{15}$$

A rough guide to when these δ_μ corrections can be neglected is therefore

$$\delta^j_\mu h^\tau \ll \delta^{i\tau\tau}_\lambda, \delta^{i33}_{\lambda'_\perp}\left(\frac{h_b}{h_\tau}\right). \tag{16}$$

There are also bilinear loop contributions of the form

$$[m^{loop}]_{ij} \sim [\delta^i_\mu (h^i_e)^2][\delta^j_\mu] m_{SUSY} \quad (i,j \in \{\tau,\mu,e\}). \tag{17}$$

These initially appear more significant, because they are only suppressed by two, rather than four, trilinears or Yukawas. However, $m_\nu^{loop} \ll m_\nu^{tree}$ and $\hat{\nu}^{tree} \propto (\delta^\tau_\mu, \delta^\mu_\mu, \delta^e_\mu)$, so contributions of the form of Eq. (17) mix $\hat{\nu}^{tree}$ with ν^2 and ν^1. These latter two neutrinos, which are massless at tree level, therefore acquire a seesaw mass of order

$$[m^{loop}]_{ij} \sim \sum_k \delta^i_\mu (h^i_e)^2 m_{SUSY} \frac{(\delta^k_\mu)^2}{|\delta_\mu|^2 m_{SUSY}} \times (h^j_e)^2 \delta^j_\mu m_{SUSY}$$
$$\sim [\delta^i_\mu (h^i_e)^2][(h^j_e)^2 \delta^j_\mu] m_{SUSY}$$
$$(i,j \in \{\tau,\mu,e\}). \tag{18}$$

[6]We are neglecting flavor violation among the sneutrinos, which could induce a significant loop mass even if $\vec{B} \simeq b\vec{\mu}$ [21].

This is the mass matrix structure we considered before Eq. (15), and will make a significant contribution if Eq. (15) is satisfied. So Eq. (15) is the condition for when δ_μ bilinears should be included in loops, or equivalently, Eq. (16) is a rough estimate of when the δ_μ loops can be neglected.

IV. PHENOMENOLOGY

In this section we briefly consider the constraints that can be set on $R\!\!\!/_p$ couplings from solar and atmospheric neutrino data. We follow the approach of Refs. [22,23], who set bounds on $R\!\!\!/_p$ models corresponding to case A—models where the bilinears are negligible in loops and neutrino loop masses are due to trilinear couplings. We discuss here a toy model where the $R\!\!\!/_p$ is in the bilinears, and the δ_B loops make a significant contribution to $[m_\nu]_{ij}$ (case B of the previous section). We leave case C—where δ_μ should be included in the loops—for a subsequent analysis [10]. We would like to establish bounds on the different set of basis independent combinations of coupling constants that contribute to the neutrino mass matrix. These bounds are more indicative of orders of magnitude than steadfast constraints. In order to proceed we make the following assumptions. First, we use the results of Ref. [22], which constrain a general 3×3 symmetric mass matrix from neutrino data considering: atmospheric and solar neutrino experiments, the CHOOZ experiment and the constraint from neutrinoless double beta decay. The overall conclusion of this analysis is that the mass matrix elements should be constrained to be on the order of $|[m_\nu]_{ij}|\lesssim 0.1$ eV. Here we present our bounds allowing each individual matrix element to take on the maximum value of 0.1 eV. This simple approach can be extended to obtain bounds when we include combinations of contributions to the neutrino mass matrix from δ^i_μ, δ^i_B, δ^{ijk}_λ, for any given model which contains these R-parity violating terms originally in the Lagrangian.

Secondly, we assume that each of the contributions from the diagrams that we have found is separately the unique contribution at a given time.[7] In this way we are trying to obtain the *weakest* constraint on the basis-independent combination of coupling constants. That is we allow each separate contribution to take on its maximum value. We can then choose from all of the bounds which is the strongest constraint on a given combinations of coupling constants. We also assume, unless otherwise indicated, that all supersymmetric mass scales are the same of order m_{SUSY}. The next approximation we make is that when we sum over neutralinos or charginos there is no suppression arising from the mixing angles. We also assume that the magnitude of all R-parity violating couplings constants to be generation blind separately. That is, all B_i to be of the same order of magnitude, and similarly for μ_i, λ_{ijk}, λ'_{ijk}, but we do not suppose beforehand that R-parity violating coupling constants arising from different terms in the Lagrangian are also of the same order of magnitude. The numerical results for all diagrams are summarized in Appendix D.

As we can see from the tables in Appendix D the strongest bounds for the combination of basis-independent coupling constants $\delta^i_B\delta^j_B$ arises from the Grossman-Haber diagram:

$$\delta^i_B\delta^j_B<3\times 10^{-10}. \tag{19}$$

For $\delta^i_B\delta^j_\mu$ the best bound comes from diagram 19, which is the neutral Grossman-Haber loop with on R-parity violation at points I and VI:

$$\delta^i_B\delta^j_\mu<7\times 10^{-10}. \tag{20}$$

(We use $\tan\beta=2$ and a generic $m_{SUSY}\sim 100$ GeV for both these bounds.) The strongest constraint on $\delta^i_\mu\delta^j_\mu$ is from the tree-level mass:

$$\delta^i_\mu\delta^j_\mu<10^{-12}. \tag{21}$$

For comparison, we list the bounds which can be derived from the remaining diagrams in Appendix D.

A. Toy model

Suppose we only allow the presence of the basis-independent combinations of coupling constants δ^i_μ and δ^i_B. A nonzero value of δ^i_μ can arise either from having $\mu_i\neq 0$ or $\langle\tilde{\nu}_i\rangle\neq 0$, so this model could arise if all the $R\!\!\!/_p$ originates in the soft SUSY breaking terms B_i, which induces a misalignment between the VEV and superpotential couplings. (This would induce $\delta_{\lambda'}\sim h_b\delta_\mu$ and $\delta_\lambda\sim h_\tau\delta_\mu$, which we neglect because we assume our model to be in case B, where contributions of this size can be neglected.) This differs slightly from the usual bilinear model, discussed in detail in [16–18], where the $R\!\!\!/_p$ originates in the GUT-scale misalignment between $\vec{\mu}$ and the trilinears, so that $\vec{B}$ becomes misaligned with respect to $\vec{\mu}$ while running down to the weak scale. From the results of Appendix D we see that the relevant contributions to the neutrino mass matrix will arise from the tree level contribution plus diagrams 3 and 19. The upper bound $\delta^i_\mu\lesssim 10^{-6}$ from the tree level mass contribution ensures that (for low $\tan\beta$) the remaining diagrams, which in principle contribute to the neutrino mass matrix through mass insertions of δ^i_μ in the loops, are negligible.

With these three contributions we can obtain neutrino masses in the phenomenologically interesting region which can simultaneously satisfy atmospheric and solar neutrino data constraints. There are several ways to see this. The full mass matrix using our simple approximations is given by

$$m^{ij}_\nu=m_{SUSY}\delta^i_\mu\delta^j_\mu+a_1 m_{SUSY}\delta^i_B\delta^j_B+a_1 m_{SUSY}\times(\delta^i_B\delta^j_\mu+\delta^j_B\delta^i_\mu), \tag{22}$$

where $a_1\simeq g^2/64\pi^2$. Certain subcases of this mass matrix can generate neutrino mass textures, which have been analyzed in the literature, that can produce neutrino masses and mixing angles in accordance with present neutrino data. As a simple example, we see that if we set $\delta^3_B=0$, and neglect the

[7]This may be incorrect in a poorly chosen basis, where different diagrams cancel each other [10].

$\delta_\mu \delta_B$ term in Eq. (22), then the structure of the neutrino mass matrix corresponds to the one analyzed in case 1 of Ref. [23]. In this case the neutrino mass matrix at one-loop consists simply of the tree-level term plus a correction to the 1-2 submatrix. The subcase analyzed in Ref. [23] had this same structure but the loop correction was due to the trilinear diagram.

It is well known that the tree level contribution can give mass to only one of the neutrinos. Together with the loop contributions one of the neutrinos will have a mass

$$m_{\nu_3} = m_{SUSY} \sum_i |\delta_\mu^i + \sqrt{a_1}\delta_{B_\parallel}^i|^2, \tag{23}$$

where we have used the decomposition $\vec{B} = \vec{B}_\perp + \vec{B}_\parallel$ of Eq. (11).

The sub-mass-matrix for the remaining two neutrinos ν^1 and ν^2 is given by

$$m_\nu^{ij} = a_1 m_{SUSY} \delta_{B_\perp}^i \delta_{B_\perp}^j . \tag{24}$$

Terms of the form $\delta_{B_\perp}^i \delta_\mu^i$ mix the heavier ν^3 and the lighter (ν^1, ν^2). It can be seen from Eq. (18) that the seesaw mass generated from this mixing is suppressed, given our choice of SUSY parameters, compared to the direct loop contribution given in Eq. (24). So in this case, this model corresponds to case 1 of [23]. This simple example[8] shows that a hierarchical neutrino mass spectrum, which satisfies atmospheric and solar neutrino data constraints, can easily be obtained by taking $|\delta_\mu + \sqrt{a_1}\delta_{B_\parallel}| \sim few \times 10^{-6}$ and $\delta_{B_\perp}^i \sim few \times 10^{-6} - 10^{-5}$. This gives us a massless neutrino and two massive neutrinos such that $\Delta m_{atm} \sim m_{\nu_3}^2$ and $\Delta m_{solar} \sim m_{\nu_2}^2$. It is also possible to obtain other types of spectra for different input values.

V. CONCLUSIONS

There are many diagrams which can contribute to the neutrino mass matrix in the framework of the MSSM without *R* parity. In general, in the literature only a few of these have been considered. In the present paper we have obtained the full analytic expression for the different diagrams contributing to the neutrino mass matrix from *R*-parity violating bilinear and trilinear coupling constants. We have expressed each contribution in terms of basis-independent combinations of couplings. We have discussed the values of the various couplings for which the separate diagrams make significant contributions to the neutrino mass matrix. We have presented bounds on combinations of the basis-independent couplings constants from neutrino experimental data, and shown that a simple toy model of bilinear *R*-parity violation can successfully accommodate the necessary mass-squared differences to account for the neutrino oscillations.

[8]We leave a more detailed numerical analysis for future work.

ACKNOWLEDGMENTS

We would like to thank Eung Jin Chun, Herbi Dreiner and Paolo Gambino for useful conversations. The work of M.L. was partially suported by Colciencias-BID, under contract no. 120-2000.

APPENDIX A: RENORMALIZATION—WHICH ARE THE FINITE LOOPS

In these appendixes we present the one loop contributions to the neutrino mass matrix, *excluding* the one-loop corrections to the tree level mass, because we are interested in the one-loop masses for the neutrinos that are massless at tree level. We identify these loops in Appendix A. In Appendix B we systematically list all diagrams and give the exact expressions that contribute to the neutrino mass, ordering them by the roman numerals that identify, in Fig. 2, where the two units of $\not{R}_p$ are. The amplitudes in Appendix B are "basis-independent," that is they are expressed in terms of invariants and MSSM parameters. Notice that the neutrino mass matrix elements are *minus* the amplitude for the diagram, $[m_\nu]_{ij} = -\mathcal{M}_{ij}(p^2=0)$, so our formulas are for $-[m_\nu]_{ij}$. We present the $\not{R}_p$ Feynman rules in Appendix C. Appendix D contains our numerical results for bounds placed on combinations of basis-independent couplings constants from neutrino data.

We wish to neglect loop corrections to the tree level mass, because we do not need such accuracy and because we prefer to avoid the issue of renormalization. We therefore neglect all diagrams involving gauge bosons and those with $\not{R}_p$ at I and VIII. We initially expected the remaining loops to be finite, because they could contribute mass to the neutrinos who are massless at tree level. However, diagram 17 [Fig. 2(d) with $\not{R}_p$ at I and VII] is renormalization scale (Q^2) dependent. In this appendix we show that the offending Q^2-dependent diagram is a loop correction to the tree mass.

The tree mass matrix can be written

$$[m_\nu]_{ij} = m_3^{tree} (\hat{e}_3^{tree})_i (\hat{e}_3^{tree})_j \tag{A1}$$

where $\hat{e}_3^{tree}$ is the eigenvector associated with m_3^{tree}. At one loop, both the mass and eigenvector are modified:

$$[m_\nu]_{ij} = (m_3^{tree} + \Delta m_3)(\hat{e}_3^{tree} + \Delta\hat{e}_3)_i (\hat{e}_3^{tree} + \Delta\hat{e}_3)_j . \tag{A2}$$

We do not want to include loops contributing to Δm_3 or $\Delta\hat{e}_3$. We do not calculate gauge loops and diagrams with $\not{R}_p$ at I and VIII, which contribute to Δm_3. However, there are also loop corrections which change the direction of $\hat{e}_3$, that is loop corrections to the angles in the rotation matrix which diagonalizes the 7×7 neutral fermion mass matrix. These loops are included in our calculation, and we want to identify them and throw them out.

We work in the mass insertion approximation, in the flavor basis where $(\hat{L}_l)^J \propto \lambda^{JKl} v_K$. This is the basis where the charged lepton mass matrix is diagonal in the MSSM. Some care is required in determining the $\{v_I\}$. For one-loop neutrino masses, it is sufficient to use the VEV $\{v_I\}$ that minimize the tree level potential. To identify the one-loop corrections to the tree mass, we must use some one-loop choice for the $\{v_I\}$. There are various possibilities, for instance, we could use the VEVs that minimize the one-loop effective potential, or we could use the tree + one-loop masses that mix neutrinos and $\tilde{h}_d^o$ with gauginos. We opt for the latter, because in such a basis it is easy to separate the loop corrections to $m_3\hat{e}_3^T\hat{e}_3$ from the loop masses m_2 and m_1. So we choose a basis where there are no tree and one-loop mass terms mixing $\tilde{w}^o$ with ν_i. This means that there will be small tree-level sneutrino VEVs which cancel the one-loop $\tilde{w}^o\nu_i$ mass. These VEVs are formally of one loop order, so are irrelevant inside the loops, because their contribution would be of two loop order. The contribution of these sneutrino VEVs to the numerical value of the tree level mass is also a higher order effect and therefore negligible. The one place these VEVs must be included is in the one-loop $\nu_i\tilde{b}_o$ mass, where the tree level sneutrino VEV contribution (formally one loop order) cancels the scale dependent part of the one-loop $\nu_i\tilde{b}_o$ mass, but leaves a finite $\nu_i\tilde{b}_o$ mixing. These can contribute to the loop masses m_2 and m_1, as can loop contributions to $h_d\nu_i$ mixing.

We know that in the flavor basis at tree level the neutrino mass is given by Eq. (4). The one-loop expression will be the same, in our present basis, provided we identify the μ_i of Eq. (4) with the tree + one-loop mass terms that mix $\tilde{h}_u^o$ with ν_i. Since we are only interested in the lowest order contributions to neutrino masses, we only include the tree level contribution to m_3. Knowing the one-loop corrections allows us to identify the finite loops that generate masses m_2 and m_1: these will be loops without mass insertions on the external legs, and loops with one mass insertion that mixes a neutrino with $\tilde{h}_d$ or $\tilde{b}^o$. The loops mixing a neutrino with $\tilde{h}_d$ or $\tilde{b}^o$ are *finite* in our present basis, as we show in Appendix B, diagram 17.

In summary, we identify the loops contributing to one-loop neutrino masses m_2 and m_1 to be those without mass insertions on the external legs, and diagrams with a mass insertion on one of the legs that mixes a neutrino with the $\tilde{b}^o$ or $\tilde{h}_d^o$ components of a neutralino. The remaining loop diagrams, with a mass insertion on both external legs, or a mass insertion mixing ν_i with $\tilde{w}^o$ or $\tilde{h}_u$ are corrections to the tree mass.

APPENDIX B: BASIS-INDEPENDENT DIAGRAM AMPLITUDES

In this appendix we write the contributions to the neutrino mass matrix $[m_\nu]_{ij}$ from each diagram in terms of MSSM parameters and invariants. The latter can be evaluated in any basis.

We list all imaginable diagrams, and explain why some are zero or negligible. We write the MSSM parameters in the mass eigenstate basis (but neglecting A terms in the scalar mass matrices), with diagonal quark and charged lepton mass matrices. See Appendix C for definitions of the matrices Z, U, V, L, E, Q, and D which respectively rotate the neutralinos, negative charginos, positive charginos, doublet charged sleptons, singlet sleptons, down-type doublet quarks and singlet down quarks from the interaction to the mass eigenstate basis.

We define

$$\tilde{A}^{ml} = -\hat{L}_M^m\left((\lambda A)^{IMl}\frac{v_I}{\sqrt{2}} + \mu_I\frac{v_u}{\sqrt{2}}\lambda^{IMl}\right), \tag{B1}$$

with $\hat{L}^m = \lambda^m\cdot\vec{v}/|\lambda^m\cdot\vec{v}|$, see Eq. (3). Similarly we define

$$\tilde{A}_d^{ml} = -\left((\lambda' A)^{Iml}\frac{v_I}{\sqrt{2}} + \mu_I\frac{v_u}{\sqrt{2}}\lambda'^{Iml}\right). \tag{B2}$$

Notice that the indices on $\tilde{A}$ and $\tilde{A}_d$ are in the charged lepton and down quark mass eigenstate basis, respectively.

We also define

$$I(m_1,m_2) = -\frac{1}{16\pi^2}\frac{m_1^2}{m_1^2-m_2^2}\ln\frac{m_1^2}{m_2^2}, \tag{B3}$$

$$I(m_1,m_2,m_3) = \int\frac{d^4k}{(2\pi)^4}\frac{1}{k^2+m_1^2}\frac{1}{k^2+m_2^2}\frac{1}{k^2+m_3^2}$$
$$= \frac{1}{m_1^2-m_2^2}[I(m_1,m_3)-I(m_2,m_3)], \tag{B4}$$

$$I(m_1,m_2,m_3,m_4) = \frac{1}{m_1^2-m_2^2}\left[\frac{1}{m_1^2-m_3^2}[I(m_1,m_4) - I(m_3,m_4)] - \frac{1}{m_2^2-m_3^2}\times[I(m_2,m_4)-I(m_3,m_4)]\right], \tag{B5}$$

$$I(m_1,m_2,m_3,m_4,m_5) = \frac{1}{m_1^2-m_2^2}[I(m_1,m_3,m_4,m_5) - I(m_2,m_3,m_4,m_5)]. \tag{B6}$$

1. λ−λ diagrams—Fig. 2(a)

R_p violation at (I,VIII): this is a loop correction to the tree mass, so it can be neglected.

R_p violation at (I,VII) and (II,VIII) (diagram 6)

$$(I,VII)+(II,VIII)=\sum_{\alpha,l,k,m,p,n,q}\delta^i_\mu\delta^{qjn}_\lambda m_{e_n}h^n_e|\mu|\tilde{A}^{kp}\times E_{nl}E^*_{pl}L_{qm}L^*_{km}\times\frac{Z^*_{\alpha3}Z^*_{\alpha4}}{m_{\chi^o_\alpha}}I(m_{e_n},m_{\tilde{E}_l},m_{\tilde{L}_m})+(i\leftrightarrow j). \tag{B7}$$

R_p violation at (I,VI) (diagram 11)

$$(I,VI)=-\sum_{\alpha,l,p,r,q}\delta^i_\mu\delta^m_B(h^j_e)^2m_{e_j}\tilde{A}^{qp}|B||\mu|\times E_{jl}E^*_{pl}L_{mr}L^*_{qr}\tan\beta\frac{Z^*_{\alpha3}Z^*_{\alpha4}}{m_{\chi^o_\alpha}}\times I(m_{e_j},m_{\tilde{E}_l},m_{\tilde{L}_r},m_{H^-})+(i\leftrightarrow j). \tag{B8}$$

R_p violation at (I,V) (diagram 7)

$$(I,V)=-\sum_{\alpha,l,k}\delta^i_\mu|\mu|^2(h^j_e)^2m^j_em^k_e\delta^k_\mu\sin^2\beta\tan\beta\times E_{jl}E^*_{kl}\frac{Z^*_{\alpha3}Z^*_{\alpha4}}{m_{\chi_\alpha}}I(m_{e_j},m_{\tilde{E}_l},m_{H^+})+(i\leftrightarrow j). \tag{B9}$$

R_p violation at (I,IV). This is not possible, because there is no R_p-violating mass involving two E^c.

R_p violation at (I,II). This is not possible; $\not{R}_p$ at II requires three incident leptons.

R_p violation at (II,VIII). This is included with R_p violation at (I,VII).

R_p violation at (II,VII) from λ couplings (diagram 1)

$$(II,VII)=-\sum_{l,m,n,r,p,q,s}\delta^{inm}_\lambda\delta^{rjn}_\lambda m_{e_n}\tilde{A}^{sq}E_{mp}E^*_{pq}\times L^*_{sl}L_{rl}I(m_{e_n},m_{\tilde{E}_p},m_{\tilde{L}_l})+(i\leftrightarrow j). \tag{B10}$$

R_p violation at (II,VI) (diagram 5)

$$(II,VI)=\sum_{m,n,s,p,q,r}\delta^{ijn}_\lambda\delta^r_B|B|m_{e_j}h^j_e\tilde{A}^{pq}\tan\beta\times E_{ns}E^*_{qs}L^*_{pm}L_{rm}I(m_{e_j},m_{\tilde{E}_s},m_{\tilde{L}_m},m_{H^+})+(i\leftrightarrow j). \tag{B11}$$

R_p violation at (II,V) (diagram 8)

$$(II,V)=-\sum_{k,l,m}\delta^{ijk}_\lambda\delta^m_\mu|\mu|m_{e_j}h^j_em_{e_m}\tan\beta\sin^2\beta\times E_{kl}E^*_{ml}I(m_{e_j},m_{\tilde{E}_l},m_{H^+})+(i\leftrightarrow j). \tag{B12}$$

R_p violation at (II,IV) is not possible because there is no $\not{R}_p$ mass between two E^c.

R_p violation at (II,III) is not possible; $\not{R}_p$ at II requires three incident leptons.

R_p violation at (III,VIII) (diagram 10)

$$(III,VIII)=-\sum_{\alpha,\beta,k,l,m,q,p}\delta^m_\mu\delta^j_\mu|\mu|^2h^i_e\tilde{A}^{pq}h^m_em_{e_m}\times E_{ik}E^*_{qk}L^*_{pl}L_{ml}V^*_{\alpha2}U^*_{\alpha2}m_{\chi^+_\alpha}\times\frac{Z^*_{\beta3}Z^*_{\beta4}}{m_{\chi^o_\beta}}I(m_{e_m},m_{\tilde{E}_k},m_{\tilde{L}_l},m_{\chi^+_\alpha})+(i\leftrightarrow j). \tag{B13}$$

R_p violation at (III,VII) (diagram 12)

$$(III,VII)=\sum_{\alpha,k,l,m,n,q,p}\delta^{jnm}_\lambda\delta^m_\mu|\mu|h^i_e\tilde{A}^{qp}m_{e_m}V^*_{\alpha2}U^*_{\alpha2}\times m_{\chi^+_\alpha}L_{nl}L^*_{ql}E_{ik}E^*_{pk}I(m_{e_m},m_{\tilde{E}_k},m_{\tilde{L}_l},m_{\chi^+_\alpha})+(i\leftrightarrow j). \tag{B14}$$

R_p violation at (III,VI) (diagram 13)

$$(III,VI)=-\sum_{\alpha,k,l,m,q,p}\delta^j_\mu\delta^m_B|\mu||B|h^i_e\tilde{A}^{qp}\tan\beta h^j_em_{e_j}\times V^*_{\alpha2}U^*_{\alpha2}m^+_{\chi_\alpha}E_{ik}E^*_{pk}L^*_{ql}L_{ml}\times I(m_{e_j},m_{\tilde{E}_k},m_{\tilde{L}_l},m_{H^+},m_{\chi^+_\alpha})+(i\leftrightarrow j). \tag{B15}$$

R_p violation at (III,V) (diagram 9)

$$(III,V)=\sum_{\alpha,k,n}\delta^n_\mu\delta^j_\mu|\mu|^2\tan\beta m_{e_n}\sin^2\beta m_{e_j}h^j_eh^i_e\times E_{ik}E^*_{nk}V^*_{\alpha2}U^*_{\alpha2}m_{\chi^+_\alpha}I(m_{e_j},m_{\tilde{E}_k},m_{H^+},m_{\chi^+_\alpha})+(i\leftrightarrow j). \tag{B16}$$

R_p violation at (III,IV) is not possible because there is no $\not{R}_p$ mass involving two E_c.

R_p violation at (IV,VIII) is not possible for the same reason as (III,IV)—no diagram with E^c leaving VII and arriving at V can have R_p violation at IV, so no diagrams with $\not{R}_p$ at (IV, . . .) are possible.

R_p violation at (V,VIII) is the same as (I,V).

R_p violation at (V,VII) is the same as (II,V).

R_p violation at (V,VI) is not possible, because we cannot put two units of lepton number violations on one charged line.

R_p violation at (VI,VIII) is not possible because H^+ has no R_p conserving mass with E^c.

R_p violation at (VI,VII) is not possible because H^+ has no R_p conserving mass with E^c.

2. $\lambda'-\lambda'$ diagrams—Fig. 2(b)

R_p violation at (I,VIII) is a loop correction to the tree mass.

R_p violation at (I,VII) and (II,VIII) from λ' couplings (diagram 4)

$$(I,VII)+(II,VIII)=3\sum_{\alpha,l,k,m,q,p,r}\delta^i_\mu|\mu|\frac{Z^*_{\alpha3}Z^*_{\alpha4}}{m_{\chi_\alpha}}h^k_d m_{d_k}\times\delta^{jrk}_{\lambda'}D_{kl}D^*_{ql}Q^*_{pm}Q_{rm}\tilde{A}^{pq}_d\times I(m_{d_k},m_{\tilde{D}_l},m_{\tilde{Q}_m})+3\sum_{\alpha,l,k,m,q,p,r}\delta^j_\mu|\mu|\frac{Z^*_{\alpha3}Z^*_{\alpha4}}{m_{\chi_\alpha}}h^k_d m_{d_k}\times\delta^{irk}_{\lambda'}D_{kl}D^*_{ql}Q^*_{pm}Q_{rm}\tilde{A}^{pq}_d\times I(m_{d_k},m_{\tilde{D}_l}.m_{\tilde{Q}_m}). \quad (B17)$$

R_p violation at II and VII from λ' couplings (diagram 2)

$$(II,VII)=-3\sum_{l,k,m,n,p,r,s}\delta^{ilp}_{\lambda'}\delta^{jnl}_{\lambda'}m_{d_l}\tilde{A}^{sr}_d D_{pk}D^*_{rk}Q_{nm}\times Q^*_{sm}I(m_{d_l},m_{\tilde{D}_k},m_{\tilde{Q}_m})+(i\leftrightarrow j). \quad (B18)$$

Lepton number violation is not possible inside a squark loop, so the only additional effect that bilinear $\not{R}_p$ can have is to induce squark flavor violation at V. We neglect this because the squark flavor violation is small: $\delta^i_\mu\delta^{ipq}_{\lambda'}|\mu|v_u$. If we take $m_\nu\lesssim$ eV then this implies $\delta^i_\mu\lesssim10^{-5}$, so $\delta^i_\mu\delta^{ipq}_{\lambda'}|\mu|v_u\lesssim\delta^{ipq}_{\lambda'}$ GeV^2, which is negligible. We differ here from Ref. [20], where this flavor violation due to the bilinears is included, but bilinear lepton number violation is not.

3. The Grossman-Haber diagrams—Fig. 2(c)

R_p violation at (I,VIII) is a loop correction to the tree level mass, so it is negligible.

R_p violation at (I,VI) and (IV,VIII) (diagram 19). We neglected this diagram in our previous paper—the expression for the amplitude is lengthy. In the interaction eigenstate basis, the incident neutrino can turn into an up-type Higgsino/down-type Higgsino (gaugino), which subsequently turns into a gaugino and up/down Higgs boson (an up- or down-type Higgs boson and Higgsino) at the vertex II. In mass eigenstate basis, these possibilities generate a number of terms:

$$(I,VI)+(IV,VIII)=\sum_{\alpha,\beta,l,m}\frac{g^2L^*_{jl}}{4\cos\beta}\delta^i_\mu|\mu|\frac{Z^*_{\alpha3}}{m_{\chi^o_\alpha}}m_{\chi^o_\beta}(Z^*_{\beta2}-Z^*_{\beta1}g'/g)\,\delta^m_B L_{ml}|B|\{-[Z^*_{\alpha4}(Z^*_{\beta2}-Z^*_{\beta1}g'/g)\sin\alpha+(Z^*_{\alpha2}-Z^*_{\alpha1}g'/g)Z^*_{\beta3}\cos\alpha+(Z^*_{\alpha2}-Z^*_{\alpha1}g'/g)Z^*_{\beta4}\sin\alpha]\cos(\alpha-\beta)I(m_h,m_{\chi^o_\beta},m_{\tilde{\nu}_l})+[Z^*_{\alpha4}(Z^*_{\beta2}-Z^*_{\beta1}g'/g)\cos\alpha-(Z^*_{\alpha2}-Z^*_{\alpha1}g'/g)Z^*_{\beta3}\sin\alpha+(Z^*_{\alpha2}-Z^*_{\alpha1}g'/g)Z^*_{\beta4}\cos\alpha]\times\sin(\alpha-\beta)I(m_H,m_{\chi^o_\beta},m_{\tilde{\nu}_l})-[Z^*_{\alpha4}(Z^*_{\beta2}-Z^*_{\beta1}g'/g)\sin\beta+(Z^*_{\alpha2}-Z^*_{\alpha1}g'/g)Z^*_{\beta3}\cos\beta+(Z^*_{\alpha2}-Z^*_{\alpha1}g'/g)Z^*_{\beta4}\sin\beta]I(m_A,m_{\chi^o_\beta},m_{\tilde{\nu}_l})\}+(i\leftrightarrow j). \quad (B19)$$

R_p violation at (IV,VI) (diagram 3)

$$(IV,VI)=\sum_{\alpha,l,m,k,n}\frac{g^2\delta^m_B\delta^n_B\ |B|^2}{4\cos^2\beta}(Z^*_{\alpha2}-Z^*_{\alpha1}g'/g)^2m_{\chi^o_\alpha}\times L^*_{il}L_{ml}L^*_{jk}L_{nk}\{I(m_h,m_{\tilde{\nu}_l},m_{\tilde{\nu}_k},m_{\chi^o_\alpha})\times\cos^2(\alpha-\beta)+I(m_H,m_{\tilde{\nu}_l},m_{\tilde{\nu}_k},m_{\chi^o_\alpha})\times\sin^2(\alpha-\beta)-I(m_A,m_{\tilde{\nu}_l},m_{\tilde{\nu}_k},m_{\chi^o_\alpha})\}. \quad (B20)$$

4. $g-\lambda$ and $g-\lambda'$ diagrams—Fig. 2(d)

We also include here the $g-\lambda'$ loop, with sleptons and leptons replaced by squarks and quarks in Fig. 2(d).

R_p violation at (I, VIII) would be a loop correction to the tree level mass, so is negligible.

R_p violation at (I,VII) (diagram 17). This diagram, with the $\not{R}_p$ at I removed, corresponds to a mass mixing $\tilde{w}^o\nu$, or $\tilde{b}\nu$. It is naively Q^2 (scale) dependent—see the discussion in Appendix A. We want to show that in the basis where $\tilde{w}^o\nu$ masses are zero at one loop, the $\tilde{b}\nu$ mass is finite. The basis we want is where the tree level $\tilde{w}^o\nu$ mass $(=g\langle\tilde{\nu}_i\rangle/2)$ cancels the loop $\tilde{w}^o\nu$ mass—so in this basis the $\tilde{b}\nu$ mass is $-g'\langle\tilde{\nu}_i\rangle/2+$ loop $=g'Z^*_{\alpha1}$(the $\tilde{w}^o\nu$ loop)$/gZ^*_{\alpha2}+$ the $\tilde{b}^o\nu$ loop, which is finite. $\tilde{w}^o\nu$ mixing gives:

$$(I,VII)=-\sum_{\alpha,k,l,m}\frac{gL^*_{kl}}{\sqrt{2}}m_{e_k}|\mu|\delta^i_\mu\frac{Z^*_{\alpha3}Z^*_{\alpha2}}{m_{\chi^o_\alpha}}L_{ml}\delta^{mjk}_\lambda B_0(0,m_{e_k},m_{\tilde{L}_l})$$
$$-3\sum_{\alpha,k,l,m}\frac{gQ^*_{kl}}{\sqrt{2}}m_{d_k}|\mu|\delta^i_\mu\frac{Z^*_{\alpha3}Z^*_{\alpha2}}{m_{\chi^o_\alpha}}Q_{ml}\delta^{jmk}_{\lambda'}B_0(0,m_{d_k},m_{\tilde{Q}_l})+(i\leftrightarrow j) \tag{B21}$$

and $\tilde{b}-\nu$ mixing gives

$$-\sum_{\alpha,k,l,m}m_{e_k}|\mu|\delta^i_\mu\frac{Z^*_{\alpha3}Z^*_{\alpha1}}{m_{\chi^o_\alpha}}\left\{\frac{g'L^*_{kl}L_{ml}}{\sqrt{2}}\delta^{njk}_\lambda B_0(0,m_{e_k},m_{\tilde{L}_l})-2\frac{g'E^*_{kl}E_{ml}}{\sqrt{2}}\delta^{kjm}_\lambda B_0(0,m_{e_k},m_{\tilde{E}_l})\right\}$$
$$-3\sum_{\alpha,k,l}m_{d_k}\mu_i\frac{Z^*_{\alpha3}Z^*_{\alpha1}}{m_{\chi^o_\alpha}}\left\{\frac{g'Q^*_{kl}Q_{ml}}{\sqrt{2}}\delta^{jmk}_{\lambda'}B_0(0,m_{d_k},m_{\tilde{Q}_l})-2\frac{g'D^*_{kl}D_{ml}}{\sqrt{2}}\delta^{jkm}_{\lambda'}B_0(0,m_{d_k},m_{\tilde{D}_l})\right\}+(i\leftrightarrow j). \tag{B22}$$

Using $B_0(p^2=0,m_1,m_2)=I(m_2,m_1)-\ln(m_1^2/Q^2)+1$, one can see that the finite contribution to $\tilde{b}-\nu$ mixing, which can contribute to the loop neutrino masses m_2 and m_1 is the sum of the above two expressions (B21),(B22) with $B_0(p^2=0,m_1,m_2)\rightarrow I(m_2,m_1)$:

$$(I,VII)=-\sum_{\alpha,k,l,m}\frac{g'}{\sqrt{2}}m_{e_k}\delta^i_\mu|\mu|\frac{Z^*_{\alpha3}Z^*_{\alpha1}}{m_{\chi^o_\alpha}}\{2\delta^{mjk}_\lambda L^*_{kl}L_{ml}I(m_{\tilde{L}_l},m_{e_k})-2\delta^{kjm}_\lambda E^*_{kl}E_{ml}I(m_{\tilde{E}_l},m_{e_k})\}$$
$$-3\sum_{\alpha,k,l,m}\frac{g'}{\sqrt{2}}m_{d_k}\delta^i_\mu|\mu|\frac{Z^*_{\alpha3}Z^*_{\alpha1}}{m_{\chi^o_\alpha}}\{2\delta^{jmk}_{\lambda'}Q^*_{kl}Q_{ml}I(m_{\tilde{Q}_l},m_{d_k})-2\delta^{jkm}_{\lambda'}D^*_{kl}D_{ml}I(m_{\tilde{D}_l},m_{d_k})\}+(i\leftrightarrow j). \tag{B23}$$

$R\!\!\!/_p$ at (I,V) (diagram 20). The particle labels in Fig. 2(d) do not apply in this case. The incident ν_i mixes with a gaugino, and the internal fermion line is a Higgsino, or ν_i mixes with $\tilde{h}_u$ and meets $\tilde{w}^+$ at II. The scalar incident at VII is an E^c,

$$(I,V)=-\sum_{\alpha,\beta,l,m}\delta^i_\mu\delta^m_\mu|\mu|^2\frac{g}{\sqrt{2}}\frac{Z^*_{\alpha3}}{m_{\chi^o_\alpha}}\{(Z^*_{\alpha2}+Z^*_{\alpha1}g'/g)U^*_{\beta2}V^*_{\beta2}+Z^*_{\alpha3}U^*_{\beta2}V^*_{\beta1}\}$$
$$\times m_{\chi^+_\beta}m_{e_m}h^j_e\sin^2\beta\tan\beta E_{jl}E^*_{ml}I(m_{\chi^+_\beta},m_{\tilde{E}_l},m_{H^+})+(i\leftrightarrow j). \tag{B24}$$

$R\!\!\!/_p$ at (I,IV) (diagram 21). The neutrino can mix with a gaugino, then there are two possibilities, which we list separately. Firstly, the internal fermion line can be a Higgsino. An $\tilde{A}$ insertion on the scalar line ensures that the incident scalar at VII is an E^c. The second possibility is for the gaugino to interact with $l,\tilde{L}$ at II. In this case H^+ and e^c are incident at VII. A third possibility is that the incident neutrino ν_i could also mix with $\tilde{h}_u$, which meets a $\tilde{w}$ at II, and emits a H^+_u. (An $\tilde{A}$ mass insertion on the scalar line, and m_{χ^+} on the fermion line, ensures that E^c and $\tilde{h}_d$ arrive at VII.) This third possibility is a loop correction to the tree mass (the loop, without the external mass insertion, is a contribution to $\mu_i\nu_i\tilde{h}^o_u$), so we do not include it:

$$(I,IV)_1=\sum_{\beta,\alpha,l,m,p,q,r}\delta^r_B\delta^i_\mu|\mu||B|\frac{g}{\sqrt{2}}\times\frac{Z^*_{\alpha3}(Z^*_{\alpha2}+Z^*_{\alpha1}g'/g)}{m_{\chi^o_\alpha}}\times h^j_eE_{jl}E^*_{ml}\tilde{A}^{pm}L_{rq}L^*_{pq}\tan\beta\times U^*_{\beta2}V^*_{\beta2}m_{\chi^+_\beta}I(m_{\chi^+_\beta},m_{\tilde{E}_l},m_{\tilde{L}_q},m_{H^+})+(i\leftrightarrow j). \tag{B25}$$

The second possibility gives

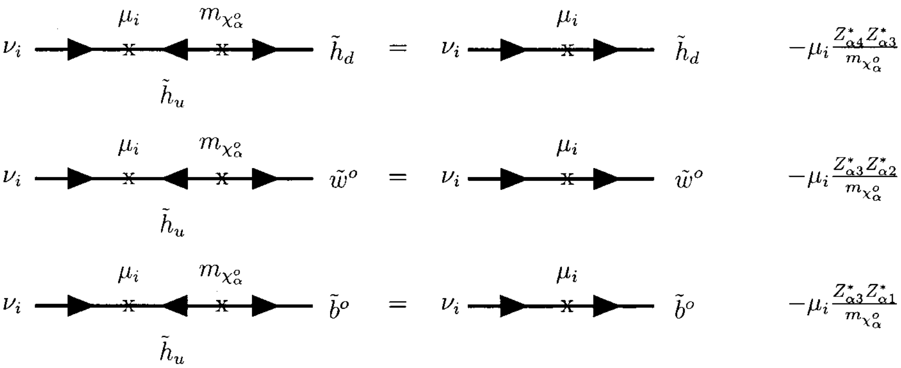

FIG. 4. Feynman rules for mass insertions on external legs. The left-hand column is a more correct representation; we use the abbrieviated notation of the central column in Fig. 2.

$$(I,IV)_2=\sum_{\alpha,m,n}\delta^i_\mu\delta^n_B|\mu||B|\frac{g}{\sqrt{2}}\frac{Z^*_{\alpha3}(Z^*_{\alpha2}+Z^*_{\alpha1}g'/g)}{m_{\chi^o_\alpha}}\times m_{e_j}h^j_e\tan\beta L_{jm}L^*_{nm}I(m_{e_j},m_{\tilde{L}_m},m_{H^+})+(i\leftrightarrow j). \quad \text{(B26)}$$

R_p violation at I and III (diagram 16). There are two possible diagrams with $\not{R}_p$ at I and III. Firstly the neutralino can arrive as a $\tilde{h}_d$ at vertex II, where a $\tilde{w}^-$ is absorbed. Secondly the neutralino can arrive as a gaugino, in which case the $\tilde{h}^-_d$ part of the chargino is absorbed,

$$(I,III)=-\sum_{\alpha\beta}\delta^i_\mu\delta^j_\mu|\mu|^2\frac{g}{\sqrt{2}}\sin^2\beta h^j_e m_{e_j}\times\left\{V^*_{\alpha2}U^*_{\alpha1}m_{\chi^+_\alpha}\frac{Z^*_{\beta3}Z^*_{\beta4}}{m_{\chi^o_\beta}}-V^*_{\alpha2}U^*_{\alpha2}m_{\chi^+_\alpha}\frac{(Z^*_{\beta2}+Z^*_{\beta1}g'/g)Z^*_{\beta3}}{m_{\chi^o_\beta}}\right\}\times I(m_{e_j},m^+_H,m^+_{\chi_\alpha})+(i\leftrightarrow j). \quad \text{(B27)}$$

R_p violation at III and VIII (diagram 15)

$$(III,VIII)=-\sum_{\alpha\beta,k,l}\delta^k_\mu\delta^j_\mu|\mu|^2\frac{g}{\sqrt{2}}L^*_{il}L_{kl}h^k_e m_{e_k}V^*_{\alpha2}U^*_{\alpha1}\times m^+_{\chi_\alpha}\frac{Z^*_{\beta3}Z^*_{\beta4}}{m^o_{\chi_\beta}}I(m_{e_k},m_{\tilde{L}_l},m_{\chi^+_\alpha})+(i\leftrightarrow j). \quad \text{(B28)}$$

R_p violation at III and VII in $g-\lambda$ loop; as noted in Ref. [11] this is zero if the sleptons are mass degenerate (diagram 18)

$$(III,VII)=\sum_{\alpha,k,l,m}\delta^k_\mu|\mu|\delta^{mjk}_\lambda\frac{g}{\sqrt{2}}m_{e_k}V^*_{\alpha2}U^*_{\alpha1}m_{\chi^+_\alpha}\times L^*_{il}L_{ml}I(m_{e_k},m_{\tilde{L}_l},m_{\chi^+_\alpha})+(i\leftrightarrow j). \quad \text{(B29)}$$

R_p violation at (III,IV) (diagram 14)

$$(III,IV)=-\sum_{\alpha,l,k}\delta^j_\mu\delta^k_B|\mu||B|\frac{g}{\sqrt{2}}U^*_{\alpha1}V^*_{\alpha2}m_{\chi^+_\alpha}m_{e_j}h^j_e\times L^*_{il}L_{kl}\tan\beta I(m_{e_j},m_{\tilde{L}_l},m_{H^+},m_{\chi^+_\alpha})+(i\leftrightarrow j). \quad \text{(B30)}$$

R_p violation at (IV,VIII) and (IV,VII) do not exist because a doublet slepton must come out of II, so no particles carrying a lepton number would arrive at VII.

R_p violation at (IV,V) and (IV,VI) do not exist because there cannot be two units of a lepton number violation on a charged line.

R_p violation at (V,VIII) and (V,VII) do not exist because a doublet slepton must come out of II, so no particles carrying a lepton number would arrive at VII.

APPENDIX C: CONVENTIONS AND FEYNMAN RULES

We take all coupling constants to be real. Indices on Yukawa couplings and A are in order doublet(d) singlet (s): h^{ds}_e. We work in the mass eigenstate basis of the charged leptons and down-type quarks, where the Yukawa couplings are diagonal and only need one index.

The MSSM neutralino mass matrix is diagonalized by the matrix Z_{mf}, with flavor eigenstate index f:1 . . . 4 corresponding to $(-i\tilde{B},-i\tilde{W}^o,\tilde{h}^o_u,\tilde{h}^o_d)$. The first index m is the mass eigenstate index. The chargino mass matrix is diago-

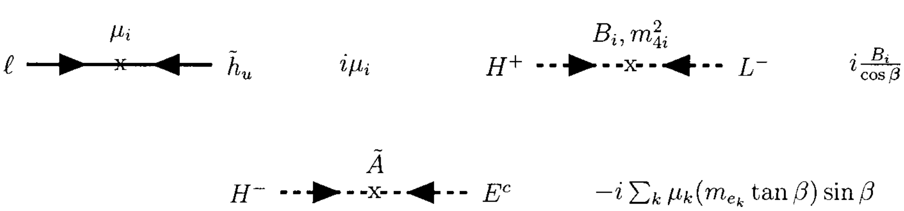

FIG. 5. Internal charged line mass insertions. Appendix C clarifies these Feynman rules.

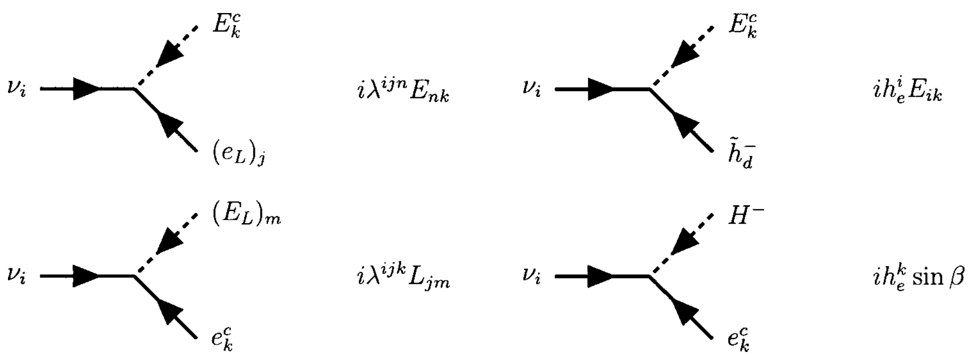

FIG. 6. Feynman rules for trilinear and Yukawa interactions. For the quarks, replace $\lambda_{ijk} \to \lambda'^{ijk}$, $E_k^c \to D_k^c$, $(e_L)_j \to (q_L)_j$, and so on.

nalized by matrices U and V: $U^* M V^\dagger = M_{diag}$, so the positive (negative) mass eigenstates are $\chi_m^+ = V_{mf}\psi_f^+$ $[\chi_m^- = U_{mf}\psi_f^-]$, where $\psi_f^+ = (-i\tilde{w}^+, \tilde{h}_u^+)$ and $\psi_f^- = (-i\tilde{w}^-, \tilde{h}_d^-)$. The doublet and singlet charged slepton (down-type quark) mass matrices are separately diagonalized by matrices L_{fm} and E_{fm} (Q_{fm} and D_{fm}), with an index order flavor eigenstate–mass eigenstate. We include the A term mixing between doublets and singlets in perturbation theory (the mass insertion approximation).

We use MSSM Feynman rules from [3], with additional Feynman rules to include the $R\!\!\!/_p$ interactions in Figs. 4, 5, and 6. Line direction is superfield chirality.

For a Lagrangian

$$\mathcal{L} = \overline{\psi}(i\partial\!\!\!/ - m)\psi, \tag{C1}$$

we fix the phase of the mass insertion to be $-i$ because

TABLE III. Numerical bounds on combinations of couplings constants under the assumption that only one diagram contributes to the neutrino mass matrix elements.

Diagram	Bound on combination of coupling constants	i/j	1	2	3
Tree − level	$\delta_\mu^i \delta_\mu^j \le 10^{-12}$.				
1	$\delta_\lambda^{ink}\delta_\lambda^{jkn} =$	1	2.7×10^{-7}	2.7×10^{-7}	4.4×10^{-6}
		2	2.7×10^{-7}	2.7×10^{-7}	4.4×10^{-6}
		3	4.4×10^{-6}	4.4×10^{-6}	7.1×10^{-5}
2	$\delta_{\lambda'}^{i33}\delta_{\lambda'}^{j33} \le 1.05\times10^{-8}$				
3	$\delta_B^i \delta_B^j \le 2.9\times10^{-10}$				
4	$(\delta_\mu^j \delta_{\lambda'}^{i33} + \delta_\mu^i \delta_{\lambda'}^{j33}) \le 3.2\times10^{-7}$.				
5	$\delta_\lambda^{ij3}\delta_B^3 =$	1	0	3.2×10^{-3}	1.2×10^{-5}
		2	3.2×10^{-3}	0	1.2×10^{-5}
		3	1.2×10^{-5}	1.2×10^{-5}	0
6	$(\delta_\mu^j \delta_\lambda^{ikk} + \delta_\mu^i \delta_\lambda^{jkk}) =$	1	2.5×10^{-5}	2.5×10^{-5}	2.5×10^{-5}
		2	2.5×10^{-5}	2.5×10^{-5}	2.5×10^{-5}
		3	2.5×10^{-5}	2.5×10^{-5}	1.0×10^{-1}
7	$\delta_\mu^i \delta_\mu^j =$	1	− − −	− − −	7.1×10^{-4}
		2	− − −	− − −	7.1×10^{-4}
		3	7.1×10^{-4}	7.1×10^{-4}	3.5×10^{-4}
8	The bounds can be obtained from the bounds of diagram5/($\sin^2\beta$).				
9	$\delta_\mu^i \delta_\mu^j =$	1	− − −	− − −	− − −
		2	− − −	− − −	9.3×10^{-2}
		3	− − −	9.3×10^{-2}	3.5×10^{-4}
10	The bounds can be obtained from diagram 7 × $\tan\beta\sin^2\beta$.				
11	The bounds can be obtained from diagram 7 × $\sin^2\beta$.				
12	The bounds can be obtained from diagram 5 × $\tan\beta$.				
13	The bounds can be obtained from diagram 9 × $\tan\beta\sin^2\beta$.				
14	$(\delta_\mu^i \delta_B^j) =$	1	− − −	1.2×10^{-4}	4.6×10^{-7}
		2	− − −	6.0×10^{-5}	4.6×10^{-7}
		3	− − −	− − −	2.3×10^{-7}
15	The bounds here can be obtained from those diagram 20 × $\tan\beta\sin^2\beta$.				
16	The bounds here can be obtained from those diagram 20 × $\tan\beta$.				
17a	$(\delta_\mu^i \delta_\lambda^{j33} + \delta_\mu^j \delta_\lambda^{i33}) = 1.0\times10^{-8}$				
17b	$(\delta_\mu^i \delta_\lambda'^{j33} + \delta_\mu^j \delta_\lambda'^{i33}) = 3.4\times10^{-9}$				
18	This diagram is non − zero only for non − degenerate sleptons.				
19	$(\delta_\mu^i \delta_B^j + \delta_\mu^j \delta_B^i) = 6.7\times10^{-10}$				
20	$\delta_\mu^i \delta_\mu^j =$	1	− − −	1.5×10^{-4}	5.7×10^{-7}
		2	1.5×10^{-4}	7.5×10^{-5}	5.7×10^{-7}
		3	5.7×10^{-7}	5.7×10^{-7}	2.8×10^{-7}
21	The bound of diagram 14 on $\delta_\mu^i \delta_B^j$ applies to $\delta_\mu^j \delta_B^i$.				

$$\frac{i}{\not p - m} = \frac{i}{\not p} + \frac{i}{\not p}(-im)\frac{i}{\not p} + \ \ldots \ . \tag{C2}$$

The $-i\mu_i$ mass insertions on the external legs of the diagram mix the incident flavor eigenstate neutrino ν_i with the $\tilde{h}_u^o$ component of a neutralino. So the external leg propagator delivering a flavor eigenstate neutralino f to vertex II is

$$\frac{i}{\not p}(-i\mu_i)\sum_\alpha \frac{iZ^*_{\alpha 3}Z^*_{\alpha f}}{\not p - m_{\chi^o_\alpha}} = \frac{i}{\not p}(-\mu_i)\sum_\alpha \left(\frac{Z^*_{\alpha 3}Z^*_{\alpha f}}{m_{\chi^o_\alpha}}\right), \tag{C3}$$

where we have used $p^2=0$. This gives the Feynman rules of Fig. 4.

The R_p-violating μ_i and B_i mass insertions, and the $\tilde{A}$ mass insertion, on internal charged lines are negative [by SU(2) antisymmetric contraction], so they effectively appear in the amplitude with a negative sign:

$$\frac{i}{\not p - m_1}(i|\mu_i|)\frac{i}{\not p - m_2} = \frac{i}{\not p - m_1}\frac{-|\mu_i|}{\not p - m_2}. \tag{C4}$$

(However, the $\not R_p$ part of $\tilde{A}$ is $-\lambda^{i4i}\mu_i v_u/\sqrt{2} = m_{e_i}\mu_i \tan\beta$, so it appears positive in the amplitude.)

The Feynman rule we quote in Fig. 5 for the mass insertion B_i also includes the effect of the soft mass m^2_{4i}. The minimization condition for the potential, in the $\langle\tilde{\nu}_i\rangle=0$ basis, implies that $m^2_{4i}=-B_i\tan\beta$ (at arbitrary loop order) [19], so the $\not R_p$ mixing between H^- and L is

$$-B_i\cos\beta + m^2_{4i}\sin\beta = -\frac{B_i}{\cos\beta}. \tag{C5}$$

APPENDIX D: NUMERICAL BOUNDS

In this appendix we summarize the numerical bounds for each diagram. We emphasize that we make the assumptions described in Sec. IV in order that the combination of couplings constants are allowed the largest possible values. It is easy to see that under these assumptions the integrals that appear in the expressions of Appendix B can be simply replaced by

$$I(m_1,m_2,m_3)\to\frac{1}{16\pi^2}\frac{1}{m^2_{SUSY}},$$

$$I(m_1,m_2,m_3,m_4)\to\frac{1}{16\pi^2}\frac{1}{m^4_{SUSY}},$$

$$I(m_1,m_2,m_3,m_4,m_5)\to\frac{1}{16\pi^2}\frac{1}{m^6_{SUSY}}. \tag{D1}$$

The results are given in Table III. For all bounds we use $|m_\nu|$, $m_{SUSY}=100$ GeV and $\tan\beta=2$. For diagram 14 the i index on δ_μ corresponds to the column, and the j index to the row. The dashes indicate that there is no bound.

[1] See for example and references therein: R. Barbieri, J. Ellis, and M.K. Gaillard, Phys. Lett. **90B**, 249 (1980); M. Gell-Mann, P. Ramond, and R. Slansky, in *Supergravity*, Proceedings of the Supergravity Workshop, Stony Brook, New York, 1979, edited by P. van Nieuwenhuizen and D. Freedman (North-Holland, Amsterdam, 1979); T. Yanagida, in *Proceedings of the Workshop on Unified Theories and Baryon Number in the Universe*, Tsukuba, Japan, 1979, edited by O. Sawada and A. Sugamoto (KEK, Tsukuba, 1971); S. Dimopoulos, L.J. Hall, and S. Raby, Phys. Rev. Lett. **68**, 1984 (1992); G.K. Leontaris *et al.*, Phys. Rev. D **53**, 6381 (1996); S. Lola and J.D. Vergados, Prog. Part. Nucl. Phys. **40**, 71 (1998); G. Altarelli and F. Feruglio, hep-ph/9905536; G. Altarelli, F. Feruglio, and I. Masina, Phys. Lett. B **472**, 382 (2000); J.A. Casas *et al.*, Nucl. Phys. **B569**, 82 (2000); J. High Energy Phys. **09**, 015 (1999); M. Carena *et al.*, Eur. Phys. J. C **12**, 507 (2000); P. Langacker, Nucl. Phys. B (Proc. Suppl.) **77**, 241 (1999); Z. Berezhiani and A. Rossi, J. High Energy Phys. **03**, 002 (1999).

[2] For a review, see, e.g., H.P. Nilles, Phys. Rep. **110**, 1 (1984); R. Barbieri, Riv. Nuovo Cimento **11**, 1 (1988).

[3] H.E. Haber and G.L. Kane, Phys. Rep. **117**, 75 (1985).

[4] G.R. Farrar and P. Fayet, Nucl. Phys. **B76**, 575 (1978).

[5] Super-Kamiokande Collaboration, Y. Fukuda *et al.*, Phys. Lett. B **433**, 9 (1998); **436**, 33 (1998); Phys. Rev. Lett. **81**, 1562 (1998); IMB Collaboration, R. Becker-Szendy *et al.*, Nucl. Phys. B (Proc. Suppl.) **38**, 331 (1995); Soudan-2 Collaboration, W.W.M. Allison *et al.*, Phys. Lett. B **391**, 491 (1997); **449**, 137 (1999); Kamiokande Collaboration, Y. Fukuda *et al.*, *ibid.* **335**, 237 (1994); R. Davis *et al.*, Phys. Rev. Lett. **21**, 1205 (1968); B.T. Cleveland *et al.*, Astrophys. J. **496**, 505 (1998); W. Hampel *et al.*, Phys. Lett. B **388**, 384 (1996); D.N. Abdurashitov *et al.*, Phys. Rev. Lett. **77**, 4708 (1996); **83**, 4686 (1999); Kamiokande Collaboration, K.S. Hirata *et al.*, *ibid.* **77**, 1683 (1996); Super-Kamiokande Collaboration, Y. Fukuda *et al.*, *ibid.* **81**, 1158 (1998).

[6] H.P. Nilles and N. Polonsky, Nucl. Phys. **B499**, 33 (1997); T. Banks, Y. Grossman, E. Nardi, and Y. Nir, Phys. Rev. D **52**, 5319 (1995); F.M. Borzumati, Y. Grossman, E. Nardi, and Y. Nir, Phys. Lett. B **384**, 123 (1996); E. Nardi, Phys. Rev. D **55**, 5772 (1997).

[7] L. Hall and M. Suzuki, Nucl. Phys. **B231**, 419 (1984).

[8] Y. Grossman and H. Haber, Phys. Rev. Lett. **78**, 3438 (1997); Phys. Rev. D **59**, 093008 (1999); hep-ph/9906310.

[9] H. Dreiner, hep-ph/9707435. G. Bhattacharyya, Nucl. Phys. B (Proc. Suppl.) **52A**, 83 (1997); hep-ph/9709395; B. Allanach, A. Dedes, and H. Dreiner, Phys. Rev. D **60**, 075014 (1999).

[10] A. Abada, S. Davidson, and M. Losada, hep-ph/0111332.

[11] S. Davidson and M. Losada, J. High Energy Phys. **05**, 021 (2000).

[12] S. Davidson and J. Ellis, Phys. Lett. B **390**, 210 (1997); Phys. Rev. D **56**, 4182 (1997); S. Davidson, Phys. Lett. B **439**, 63 (1998).
[13] J. Ferrandis, Phys. Rev. D **60**, 095012 (1999).
[14] Y. Grossman and H. Haber, Phys. Rev. D **63**, 075011 (2001).
[15] L.J. Hall, V.A. Kostelecky, and S. Raby, Nucl. Phys. **B267**, 415 (1986).
[16] R. Hempfling, Nucl. Phys. **B478**, 3 (1996).
[17] Eung Jin Chun and Sin Kyu Kang, Phys. Rev. D **61**, 075012 (2000).
[18] M. Hirsch, M.A. Diaz, W. Porod, J.C. Romao, and J.W.F. Valle, Phys. Rev. D **62**, 113008 (2000).
[19] S. Davidson, M. Losada, and N. Rius, Nucl. Phys. **B587**, 118 (2000).
[20] O.C.W. Kong, J. High Energy Phys. **09**, 037 (2000).
[21] S. Davidson and S. King, Phys. Lett. B **445**, 191 (1998).
[22] A. Abada and M. Losada, Nucl. Phys. **B585**, 45 (2000).
[23] A. Abada and M. Losada, Phys. Lett. B **492**, 310 (2000).
[24] R. Godbole, P. Roy, and X. Tata, Nucl. Phys. **B401**, 67 (1993); M. Nowakowski and A. Pilaftsis, *ibid.* **B461**, 19 (1996); B. de Carlos and P. White, Phys. Rev. D **54**, 3427 (1996); A.Y. Smirnov and F. Vissani, Nucl. Phys. **B460**, 37 (1996); D.E. Kaplan and A.E. Nelson, J. High Energy Phys. **01**, 033 (2000); E.J. Chun and J.S. Lee, Phys. Rev. D **60**, 075002 (1999); V. Bednyakov, A. Faessler, and S. Kovalenko, Phys. Lett. B **442**, 203 (1998); J.C. Romão, Nucl. Phys. B (Proc. Suppl.) **81**, 23 (2000); S.Y. Choi, E.J. Chun, S.K. Kang, and J.S. Lee, Phys. Rev. D **60**, 075002 (1999); M. Dress, S. Pakvasa, X. Tata, and T. ter Veldhuis, *ibid.* **57**, 5335 (1997); S. Rakshit, G. Bhattacharyya, and A. Raychadhuri, *ibid.* **59**, 091701(R) (1998); G. Bhattacharyya, H.V. Klapdor-Kleingrothaus, and H. Pas, Phys. Lett. B **463**, 77 (1999); S. Bergmann, H.V. Klapdor-Kleingrothaus, and H. Pas, Phys. Rev. D **62**, 113002 (2000); E.J. Chun, S.K. Kang, C.W. Kim, and J.S. Lee, Nucl. Phys. **B544**, 89 (1999); K. Choi, E.J. Chun, and K. Hwang, Phys. Rev. D **60**, 031301(R) (1999); O.C.W. Kong, Mod. Phys. Lett. A **14**, 903 (1999); E. Ma, Phys. Rev. D **61**, 033012 (2000); A. Joshipura and S. Vempati, *ibid.* **60**, 111303(R) (1999); A. Joshipura, V. Ravindran, and S. Vempati, Phys. Lett. B **451**, 98 (1999); A. Joshipura and M. Nowakowshi, Phys. Rev. D **51**, 2421 (1995); A. Datta, B. Mukhopadhyaya, and S. Roy, *ibid.* **61**, 055006 (2000); F. Takayama and M. Yamaguchi, Phys. Lett. B **476**, 116 (2000); N. Haba, M. Matsuda, and M. Tanimoto, *ibid.* **478**, 351 (2000); B. Mukhopadhyaya, S. Roy, and F. Vissani, *ibid.* **443**, 191 (1998); K. Choi and E.J. Chun, *ibid.* **488**, 145 (2000); J. Mira, E. Nardi, D. Restrepo, and J. Valle, *ibid.* **492**, 81 (2000); K. Cheung and O.C.W. Kong, Phys. Rev. D **61**, 113012 (2000); Kiwoon Choi, Eung Jin Chun, and Kyuwan Hwang, Phys. Lett. B **488**, 145 (2000).